LATE-HOLOCENE EVOLUTION OF THE NORTHERN BAY OF CÁDIZ FROM GEOMORPHOLOGICAL, STRATIGRAPHIC AND ARCHAEOLOGICAL DATA

C. Caporizzo[1*], F.J. Gracia[2], P.P.C. Aucelli[1], L. Barbero[2], C. Martín-Puertas[3], L. Lagóstena[4], J.A. Ruiz[4], C. Alonso[5], G. Mattei[1], I. Galán-Ruffoni[2], J.A. López-Ramírez[6], A. Higueras-Milena[5],

1 Dept. of Science and Technology, Universitá degli Studi di Napoli "Parthenope", Centro Direzionale, Isola C4, 80143, Naples, Italy; pietro.aucelli@uniparthenope.it; gaia.mattei@uniparthenope.it.

2 Dept. of Earth Sciences. Facultad de Ciencias del Mar y Ambientales, Universidad de Cádiz, Puerto Real, Spain; javier.gracia@uca.es; luis.barbero@uca.es; ignacio.galanruffoni@alum.uca.es.

3 Dept. of Geography, Royal Holloway University of London, United Kingdom; celia.martinpuertas@rhul.ac.uk.

4 Dept. of History, Geography and Philosophy. Facultad de Filosofía y Letras, Universidad de Cádiz. Cádiz, Spain. lazaro.lagostena@uca.es; jantonio.ruiz@uca.es.

5 Centro de Arqueología Subacuática. Instituto Andaluz de Patrimonio Histórico. Consejería de Cultura. Junta de Andalucía, Cádiz, Spain. carlos.alonso.v@juntadeandalucia.es; aurora.h.castellano@juntadeandalucia.es.

6 Dept. of Environmental Technologies. Facultad de Ciencias del Mar y Ambientales. Universidad de Cádiz. Puerto Real, Spain. juanantonio.lopez@uca.es.

*corresponding author: claudia.caporizzo@uniparthenope.it

Abstract

The present paper deals with the historical evolution of the northern Bay of Cádiz (SW Spain) between the last eustatic maximum (6.5 ky BP) and the present day, by means of a series of independent proxies. The zone is constituted by the tidal estuary of the Guadalete River, filled with saltmarsh sediments during the late Holocene, due to the sheltering of the zone by a confining outer sandy barrier. The northern border of the Bay records an urban settlement of Phoenician age (first millennium BC), Doña Blanca. A detailed survey was made in the contact between the Phoenician city and the saltmarshes in order to detect other possible urban structures related to the morphological and sedimentary evolution of this environment during historical times. Two campaigns with GPR Stream-X array were carried out as well as aerial imaging and topographic survey with UAV. In parallel, a total of 8 boreholes were made in different parts of the saltmarshes, including radiocarbon dating of selected samples for estimating sedimentation rates in the saltmarshes. Results obtained by georadar prospection and UAV survey revealed the presence of a second urban settlement on the marginal sedimentary plain, very probably installed upon a sandy fluvial island of the Guadelete River. The urban remains, of Punic age, are partly covered by clay sediments due to the subsequent evolution of these saltmarshes, where sedimentation rates of up to nearly 2.4 mm/yr have been estimated for environments close to fluvial and/or tidal channels and hence more affected by sediment aggradation during flooding episodes. In recent times river regulation by dams and the artificial desiccation and cropping of the saltmarshes have interrupted the natural trend of the area towards sedimentary silting up.

Keywords: Holocene, environmental evolution, saltmarshes, geoarchaeology, Southern Spain

1. Introduction

Even though coastal plains and especially estuarine environments have been zones of prevalent human occupation during historical times (Allen, 2000), they are very dynamic environments due to the confluence and interaction of marine (tides, currents) and fluvial (floods) processes, where sedimentation, mainly accretion, prevails (Alberico et al., 2012; Rahman and Plater, 2014; Aranda et al., 2020). At the same time, sea-level evolution has produced changes in the areas affected by all these processes (Edwards and Horton, 2000; Pappone et al., 2012), forcing human communities to adapt to the new conditions (Fa et al., 2000; Anthony et al., 2014; Mattei et al., 2019; Bailey et al., 2020).

Reconstructing the recent evolution of such coastal environments and its interaction with human activities constitutes an imperative objective in recent and present historical and palaeoenvironmental studies (Morhange, 2000; Burningham and Cooper, 2004; Amato et al., 2011; Aucelli et al., 2016a; 2017; 2018a). However, for ancient historical times within the Holocene, available data on sea-level changes or about coastal environments different from the present ones, deduced by different kinds of sea-level proxies, provide useful information about the morpho-evolutive trends in these contexts over time (Schulz, 1983; Marriner and Morhange, 2007; Vacchi et al., 2014; 2016; Aucelli et al., 2016b; 2019a; 2019b; Khan et al., 2019; Mann et al., 2019; Ascione et al., 2020). All these aspects become more complex in tectonically active zones (Passchier et al., 2013; Amato et al., 2018; Aucelli et al., 2018b; 2018c; 2020; Pappone et al., 2019), where recent vertical movements (subsidence, tectonic rise) superimpose on the climate-eustatic and morphosedimentary trends in estuaries and low coasts (Gracia et al., 1999; 2008; Zazo et al., 1999).

Analysis of the recent Holocene evolution of tidal flats and estuaries needs a number of data coming from different sources, like the recognition, mapping and geomorphological interpretation of relict forms (Lambeck et al., 2011; Sander et al., 2016; Degeai et al., 2020), sedimentological evolution and sedimentation rates of saltmarshes (Dabrio et al., 2000; Leorri et al., 2010), or the analysis of archaeological records, both emerged and submerged (Auriemma and Solinas, 2009; Alonso and Pagés, 2010; Morhange et al., 2013; Fernandez-Montblanc et al., 2014; Aucelli et al 2016b; Mattei et al., 2018a; Giaime et al., 2019). In this sense, new microtopographic and photogrammetric techniques applied to archaeological settlements have rapidly developed in the last decade, especially with the incorporation of UAV's, unmanned aerial (and marine) vehicles (Eleveld, 2015; Fernández-Hernández et al., 2015; Mattei et al., 2018b; Aucelli et al 2020).

The Bay of Cádiz (SW Spain) constitutes an example of long historical human occupation of a typical estuarine saltmarsh environment affected by notable historical changes that have conditioned the sedimentary evolution of emerged and submerged zones (Gutiérrez-Mas et al., 2009). Supposedly, the Bay was colonized by Phoenicians in 1100 b.C. and Cádiz is considered as one of the oldest cities in western Europe (Niveau de Villedary, 2019). Within the Bay of Cádiz outstands the Phoenician settlement of Doña Blanca, one of the richest in southern Iberia. It is placed in the northern margin of the Guadalete River estuarine sedimentary flat,

historically affected by sea-level fluctuations and by an important historical sedimentary infilling, evaluable in more than 30 m of saltmarsh deposits during the Holocene (Dabrio et al., 2000).

In the last thousand years, this location has been a preferential site for the settlement of different human groups, forming communities that knew navigation techniques (Vijande et al., 2015). The survival of these groups was achieved through the exploitation of both marine (fisheries, salt harvesting) and terrestrial resources, available in the fertile low fluvial basin of the Guadalete River, close to the fluvial valley of the rich Guadalquivir River (Gracia et al., 2017). The relationships between both river valleys near the coast were frequent throughout the centuries thanks to maritime commercial activities (Alonso et al., 2009).

Doña Blanca archaeological site, located on the inner side of the bay along the banks of the Guadalete River, is one of the most important and well known Phoenician settlements in Western Mediterranean countries. According to Ruiz Mata (1999a; 1999b), the site was equipped with an ancient harbour system, although this hypothesis is still unclear since no real port remain has been identified to date. However, the study area was always investigated considering its historical evolution, but never under a palaeoenvironmental point of view.

The main goal of the present work is the study of the Holocene geomorphological evolution of the Bay and related human occupation. In this context, different techniques and data sources have been used, including geomorphological mapping, geophysical surveying with georadar, high-resolution photogrammetry and multispectral mapping with UAV's, sediment coring and radiocarbon dating of samples. The combination of all those independent data allowed proposing a palaeogeographical model of evolution and interaction between natural processes and human occupation in the northern bay of Cádiz, especially around Doña Blanca Phoenician settlement.

2. Geomorphological Setting

The Cádiz Bay (Figure 1) is located in the Guadalquivir Tertiary Depression (SW Spain), southwards of the estuary of the Guadalquivir River (Gracia et al., 1999; Alonso et al., 2015). The study area is characterized by low-lying coasts which have been affected by several important changes during the Holocene due to the development of beach ridge systems (Rodríguez-Polo et al., 2009), subject to coastal erosion and progradation episodes, mainly related to sea-level changes (Dabrio et al., 2000; Arteaga et al., 2008).

The Bay, with average length and width of 30 and 15 km respectively, is made of large marshes, extending several kilometres inland and separated from the sea by sand barrier systems, and its coast shows an average meso-tidal range of 2.1 m. Along the littoral sector the wave energy is medium (Benavente et al., 2000) and wavefronts reach the coast obliquely, due to the morphology of the shoreline, producing long-shore transport and littoral drift towards S-SE (Dabrio et al., 2000; Gracia et al., 1999).

During the Quaternary, the development of the area was connected to a convergence between Africa and Eurasia that led to the development of several strike-slip faults, still active and divided in two main families

oriented NE-SW and NW-SE that affect all the region (Gutiérrez-Mas et al., 2004; Gracia et al., 2008). This faulting system affected the distribution of emerged and submerged areas in the Bay, resulting in two main semi-circular embayments, the northern one associated with the Guadalete River estuary and saltmarshes, and the southern one forming a more open bay with saltmarshes historically transformed into Salinas (Figure 1).

While the areas tectonically elevated did not record any significant deposition during the Pleistocene, the subsiding zones between the rising blocks recorded significant sedimentary aggradation, in particular the northern part of the bay, between Puerto Real and Puerto de Santa Maria, which is covered with nearly 30 m of marsh and fluvial sediments (García de Domingo et al., 1987; Dabrio et al., 2000; Gracia et al., 2008).

Eustatic fluctuations during the middle and final stages of the Pleistocene, made alluvial plains and flooding phases evolve recording low-stands and high-stands episodes, respectively (Zazo et al., 1996; Gracia et al., 1999; 2008). During the Holocene transgression, at ca. 6.5 ky BP, the sea level reached its maximum values and flooded the ancient Pleistocene alluvial plains turning them into a marine bay roughly similar to the present one. From that moment on, the bay was subjected to a continuous sedimentary infilling, which is still active, with sediments supplied mainly by the Guadalete River (Dabrio et al., 2000; Arteaga et al., 2008; Zazo et al., 2008; Del Río et al., 2019).

After the maximum transgression, relative sea-level stability favoured the development and prograding of several spit-barrier systems, including the Valdelagrana spit-barrier, in the northern part of the bay. This littoral ridge system developed in several progradation phases (Zazo et al., 1996; Rodríguez Ramírez et al., 1996; Dabrio et al., 2000; Alonso et al., 2009; 2014; 2015; Del Río et al., 2015): a first one during Bronze Age (Borja et al., 1999) and Phoenician times (4.2-2.6 cal. ka BP and named H2 by Zazo et al., 1996), a second phase in Roman and Medieval times (2.3 - 1.1 cal. ka BP, H3) and a third phase in modern times (1.0 cal. ka BP - present, H4). An older initial phase H1, recorded in the near Doñana spit-barrier and associated Guadalquivir saltmarshes gave an age of 6.9-4.5 cal. ka BP, although it has not been identified in the Bay of Cádiz (Dabrio et al., 2000). The evolution of the Valdelagrana beach ridge system facilitated the development of a lagoonal/saltmarsh environment in the Guadalete River estuary. The inner part of the bay was, thus, mainly influenced by aggradational sedimentary processes related to tidal and fluvial processes, while the external sector of the bay, formed by sandy barriers, was more exposed to wave action.

Human interventions during roman and modern times modified the Guadalete River thalweg for navigational purposes. The San Pedro tidal channel represents the original Guadalete River mouth. The urban development of El Puerto de Santa María city during Roman times (*Portus Gaditanus*) derived in the decision of creating a direct nautical communication to the sea, by excavating a rectilinear shortage in the 1st century AD (Alonso and Gracia, 2004). The second phase of economic expansion of the city in modern times (middle 18th century; Pérez Fernández, 2018) carried out the final disconnection of the original fluvial mouth from the Roman artificial one. The result was the definitive emplacement of a unique, artificial mouth of the Guadalete River in its present location, and the abandonment of the original former one, that transformed into a wide tidal channel (the present San Pedro River) (Gracia et al., 2017). Finally, several overwash deposits located in the

143 bay were produced by historical tsunami events that affected the coasts of the Gulf of Cadiz. The most recent
144 and energetic wave events recorded in the zone took place in 2.3-1.9 cal. ka BP and in 1755 (as a consequence
145 of the destructive Lisbon earthquake). Different authors have studied in detail the effects and sedimentary and
146 morphological records of such historical events (Lario et al., 2010; Gutiérrez-Mas, 2011; Cuven et al., 2013;
147 Koster and Reicherter, 2014; Alonso et al., 2015, among others).

148

149 **3. Archaeological characterization of Doña Blanca site**

150 The Iberian Peninsula represents the most western point of the Phoenician-Punic expansion within the
151 Mediterranean region. This area was chosen as one of the first destinations during the Phoenician diaspora to
152 the West (Zamora and Sáez, 2014). The reasons behind the Spanish colonization can be attributed primarily to
153 their interest in the control and the trade of its mineral resources, namely gold, tin and, most of all, silver. Both
154 the classic historians and the archaeological remains prove that the oldest Phoenician colony in the western
155 Mediterranean was the old city of *Gadir* (present Cádiz city). In this respect, due to its strategic position, *Gadir*
156 became one of the most important trading centres from where ships easily carried products to other European
157 Atlantic and Mediterranean harbours (Ruiz Mata, 1999a; 1999b).

158 Not many Phoenician colonies were founded in the western part at the northern edge of the Gibraltar Strait and
159 the oldest one within the Bay of Cádiz is the settlement of Doña Blanca, near El Puerto de Santa María (Cádiz)
160 (Figures 1 and 2). The first excavations started in 1979 and showed traces of urbanization since the VIII century
161 BC. As proposed by Ruiz Mata et al. (2005), the ancient funding of Gadir might have been established right
162 where today Doña Blanca settlement is located. Research made at present includes three main ancient
163 settlements in the bay: Gadir (Cádiz), Cerro del Castillo (Chiclana), and Castillo de Doña Blanca (Botto, 2014).

164 The area that is now an inner site along the banks of the Guadalete River is characterised by a marshy
165 environment extending to Valdelagrana spit complex. However, during Phoenician times, it was considered as
166 an important centre, probably not far from the seaside (Ruiz Mata et al., 2005) and equipped with harbour
167 facilities, upon an ideal place for a settlement due to the proximity to the estuary of the Guadalete River.
168 According to Ruiz Mata (1999a; 1999b), the first Phoenician settlement was located at the bottom of the
169 western sector of the Sierra de San Cristóbal (Figure 1), at an altitude of 125 m, which acted as a natural barrier
170 protecting the city and the hypothetical port built in a small inlet. The Doña Blanca archaeological site is a 9
171 m thick tell including several types of remains, with different ages and characteristics (Figure 2), that reflect
172 the evolution of the Phoenician and Punic society from the VIII century BC to the Pre-Roman Age (III century
173 BC) (Ruiz Mata, 1999a; 1999b).

174 The main elements composing the archaeological site are (Ruiz Mata, 1999a; 1999b):

175 - Phoenician Block from the VIII century BC
176 - Defensive walls systems from different ages (VIII, V, IV, III centuries BC)

- Necropoli of Las Cumbres from the VIII century BC
- Village of Las Cumbres and its industrial estate (IV-III centuries BC)

The Phoenician quarter and the oldest walling structure, with an area of more than 1 km^2, belongs to the first main building phase where the walls were made with crude stones held together by lime (Ruiz Mata et al., 1998). The dwellings adapt to the steepness of the ground forming three different levels of terraces, with a climb of about 7 m. The settlement was abandoned for the first time at the end of the VIII century, because of a societal collapse of unknown origin, maybe an earthquake or a tsunami, according to some evidence found along the Gulf of Cádiz coasts (Alonso et al., 2015). This case and a similar archaeological situation in the Phoenician quarter of Gadir (Cádiz) were recently studied by Ruiz et al. (2020). Several strata of infilling covering the collapsed materials show that the settlement was occupied when a new defensive walls system was built (Ruiz Mata and Pérez, 1995). The remains of the habitations include the quadrangular floor plan, the walls and their organization, which strictly reflect their oriental origin (Pachón Veira and Manzano, 2005).

On the other hand, according to Niveau de Villedary (1995) and Ruiz Mata (1995) the village of Las Cumbres, located at the highest part of the far eastern sector of the Sierra de San Cristóbal, represents the result of the last enlargement period of the city around Doña Blanca and it accounts for 38 dwellings distributed over 1,5 km^2. The settlement is bounded on its northern side by a street and on the southern side by an open space where its industrial estate has been found. (Ruiz Mata, 2018). These urban dependencies should be complemented with the Punic harbour of La Martela (Lagóstena Barrios and Ruiz Gil, 2020) discovered in 2016 (Lagóstena Barrios et al., 2020).

4. Methods

The geoarchaeological analysis of the northern Bay of Cádiz, especially along its northern sector, was based on a number of complementary methods: geomorphological field prospections, geophysical surveys with georadar, high-resolution topographic surveys using UAV (Unmanned aerial vehicle), and coring (i.e. stratigraphic description of levels, sampling and radiocarbon datings). First of all, a geomorphological map of the northern Bay of Cádiz was reconstructed by overlaying the onsite observations with 3D vision of historical aerial photographs, accessible through the Spanish National Geographical Institute 3D visor (http.:ign.es/3d-stereo/). Special attention was paid to the oldest available flight, made by the USAF in 1956, in a period when saltmarshes showed very little artificial transformations. Spatial data were incorporated into a GIS environment (ArcMap10.4). Archaeological data obtained from previous studies and field works were also incorporated into the GIS project.

4.1 High-resolution topography and multispectral image investigations (UAV devices)

A detailed topography of the study area was produced by photogrammetric methods using images obtained with an unmanned aerial vehicle (UAV) equipped with an RGB camera. The flight was made with a DJI

Phantom 3 Professional lightweight quadricopter, with a payload of <0.5 kg, equipped with a camera with a Sony EXMOS sensor. A stabilization system (gimbal) for the camera was used. The main characteristics of the camera are: Focal length 3.1 mm; field of view FOV 94; sensor size 6.16x4.62 mm; resolution 12.76 MP; image size 4000x3000 pixels; pixel size 1,57 microns.

The work was made in the following five steps: (1) Flight planning was done using the DJI Go software, both for the definition of the flight parameters that in this case were adjusted to obtain a GSD lower than 5 cm, as well as to supply the aerial vehicle the necessary data for the automatic execution of the flight. The flight plan is represented in Figure 3. In both cases, the forward and transverse overlaps were adjusted to 80% and 60 %, respectively, and the flight altitude was set at 90 m. Also, the exposure, white balance and ISO were configured in automatic mode, as light conditions did not suffer substantial changes during the execution of the flights. (2) Data acquisition: After obtaining the corresponding permits, two flights were carried out consecutively according to the planning on the 25 March 2019, beginning at 12:30, with a duration of 8 min for the first flight and 12 min for the second one. A total of 265 and 370 images were respectively obtained, 100% of which were optimal for use in photogrammetric processing. The coordinate system used was UTM 29N WGS84 (EPSG 32,629). (3) Photogrammetric processing: At this stage, orthomosaic and 3D geometric basin model reconstruction took place through photogrammetry using structure from motion (S*f*M) algorithms. S*f*M differs from traditional photogrammetry as it does not require reference targets or a priori knowledge of the camera exposure locations and altitudes. Instead, the geometry of the camera and photographs parameters was solved automatically with very little user interaction (Madden et al., 2015). By using multiple overlapping images, S*f*M incorporates a simultaneous, highly redundant, iterative bundle adjustment procedure based on a database of features automatically extracted from a set of multiple overlapping images (Snavely et al., 2008). The camera positions derived from S*f*M lacked the scale and orientation provided by ground-control coordinates, unlike traditional photogrammetry. Consequently, the 3D point clouds were generated in a relative coordinate system (image-space), which had to be aligned to a real-world (object-space) coordinate system. The transformation of S*f*M image-space coordinates to an absolute coordinate system could be achieved using a 3D similarity transform based on a small number of known GCPs with known objects - space coordinates (Westoby et al., 2012). The processing was done using the Pix4D software with the template for 3Dmaps. The Pix4D workflow consisted of three steps: initial processing, point cloud densification, and DSM and orthomosaic generation. The user-defined properties which guide the quality, accuracy, and format of the final output were all handled through a processing options dialogue box which was set up prior to any processing steps.

Additionally, a multispectral camera onboard a fix-wing aerial system (Parrot Disco) was used to produce vegetation index maps which could contribute to the sub-surface survey. Multispectral sensor used (Micansense Sequoia) include 4 spectral bands with wave-lengths at 550, 660, 735 and 790 nm corresponding to green, red, red-edge and near infrared (NIR) parts of the electromagnetic spectrum, all with a band of 40 nm except for the red-edge which is 10 nm. The sensor is global shutter and the spectral cameras have a resolution

of 1280 x 960 pixels. Additionally, the camera mounts also a sunshine sensor, GPS and inertial unit with magnetometer for internal and external positioning of the images. Flight planning covered the same area as the previous one for photogrammetry with the necessary technical adaptation to fix-wing flight. A total of 389 images for each spectral band were acquired. Processing for producing reflectance maps for each band was made using Pix4D software. After obtaining the four reflectance maps for each spectral band, a normalised difference vegetation index (NDVI) was calculated for each pixel of the image using the following expression: NDVI = (NIR-Red)/(NIR+Red) thus producing a NDVI distribution map as will be discussed in the results section. Alternative indexes such as the green NDVI considering the green band instead of the red one were also calculated, the results being similar to the normal NDVI.

4.2 Georadar survey

The multi-channel georadar equipment used in the present research (Stream-X IDS) is composed of a set of 15 antennas (16 channels) with a central frequency of 200 MHz separated by 12 cm each. The equipment scan band has a width of 2 m. The set has a lifting system that allowed to correctly adapting the height of the antenna with respect to the prospected terrain, and a trailer system that allowed a maximum prospecting speed of 15 km per hour. The antennas were connected to a central control unit (DAD) where the data were collected. From the central unit, the system connects to a topographic precision odometer and to the laptop with the software One Vision for data acquisition and GRED HD for post-processing the data.

The georadar was configured for this work with an exploration depth of 80 ns, 512 samplings per sweep (@ 512 Sample/Scan), average propagation speed of 10 cm/ns and a GPS + PPS positioning system. The position was geo-located by a differential GPS Leica GNSS GS14 antenna with a CS15 controller, which exported the data from the receiver to the control unit in NMEA format every 0.2 sec (5 Hz).

4.3 Boreholes, stratigraphic analysis and dating

The stratigraphic dataset is composed of several boreholes performed in the zone and previously published (Dabrio et al., 2000; Arteaga et al., 2008); and new unpublished data. Stratigrapich data presented in Alonso et al. (2015) were here reinterpreted and incorporated from 58.3 m of sediments recovered from eight mechanical boreholes located between El Puerto de Santa Maria (S1, S2, S3, S4) and Puerto Real (S5, S6, S7, S8) in June 2008 (see location in Fig. 1), related to a research project elaborated by Gracia and Martín (2009). The boreholes reached depths ranging between 6 and 10 m. The obtained continuous cores were stored in appropriate coring-boxes and kept at the laboratories of the University of Cádiz. The description of the cores was carried out in three stages: initial visual description of the sediments (type, colour, presence of organic remains and organisms); detailed analysis of the sand fraction using a stereomicroscope; analysis of the clay fraction on a petrographic microscope. All the detected features were used to define different lithofacies and sedimentary units on which all the boreholes were associated. The boreholes data represented the base for the reconstruction of the late Holocene stratigraphy. Other cores made on the area, obtained by Alonso et al. (2015) were incorporated into the study and georeferenced using GIS Software (ArcMap10.4). The interpretation of

the depositional environments recorded in the cores helped to better reconstruct the ancient coastline in different morpho-evolutive scenarios. The Digital Terrain Model (DTM) of the area, with a resolution of 5 m, was downloaded from the official website of the Spanish National Geographical Institute.

Macrofossils such as fragments of shells and roots, as well as bulk sediments where macrofossils were not found, were used for radiocarbon dating at the Centro Nacional de Aceleradores (CSIC-Spain, Seville). Nine samples were taken at different depths in boreholes S1, S5, S7 and S8, in favourable levels including rests of skeletons or valves and/or organic matter, and near the main facies transitions for ^{14}C age determination. Samples were pre-treated with organic solvents and cleaning with AAA. Calibration was made according to curve INTCAL13 (probability of 95%) for sampling older than 4000 yr BP (S.7 and S.8 boreholes), and to curve Marine13 (same probability) (Reimer et al., 2013) for boreholes S.1, S.2, S.4 and S.5, younger than 4000 yr BP, by using Calib Rev. 7.0.4 software (Stuiver and Reimer, 2018). A correction had to be made due to the reservoir effect of marine radiocarbon (ΔR), very important in the coasts of the Gulf of Cádiz (Soares, 2015). In the present work, a weighted value of reservoir effect of $\Delta R = -108 \pm 31$ ^{14}C years was applied (Martins and Soares, 2013), applicable to samples younger than 4000 years, as other authors have used in later radiocarbon datings made along the Gulf of Cádiz (Soares, 2015). ΔR values depend on the specific oceanographic conditions of the place. In this sense, the South-Atlantic Spanish coast shows a negative value (-ΔR) due to the absence of wind-driven upwelling phenomena, which suggests a certain stratification of the water column (Soares and Martins, 2009). Dating results were also used for estimating Holocene sedimentation rates in the saltmarshes.

5. Results

5.1. Geomorphological analysis

The geomorphological map of the northern bay (Figure 4) shows a wide plain of sedimentary origin, surrounded by low hills. The contact between both morphological units consists of steeps slopes with some colluvial deposits (especially in the northern border) and gentle pediments (in the southern one). The tidal-fluvial sedimentary plain is partly sheltered from marine action by the Valdelagrana beach-ridge complex. Several big relict washover fans were recognized along the ridge system, probably related to past wave energetic events. The San Pedro River, as an inactive relict of the old Guadalete River channel, shows an evident deviation to the south, associated with the historical growth of the late Holocene beach ridges.

The broadly triangular shape of the fluvial deposits in the bay entrance allows mapping the zone as a palaeodelta that very probably was active in historical times, while at present is only affected by tidal processes. A wide sedimentary plain of fluvial origin spreads out between the palaeodelta and the escarpments limiting the bay to the north.

315 Regarding the fluvial-tidal plain, a distinction can be made between a clearly fluvial plain in the NW zone of
316 the bay and a more typically tidal plain in the SW zone. The fluvial plain is characterized by many remains of
317 abandoned fluvial channels associated with the Guadalete River dynamics in its entrance to the bay, where the
318 increase in the sedimentary plain width favoured rapid lateral migration of the fluvial channel. At present, the
319 plain is mainly exploited as croplands (wheat and cotton) and pastures.

320 In the tidal saltmarshes, a fully natural zone can be recognized eastward of the San Pedro River, where several
321 minor tidal channels have been mapped, mostly inactive at present. To the NW the saltmarshes were
322 historically transformed into a group of minor salinas. At present only an industrial salt harvesting exploitation
323 is functional, located in the zone where the artificial disconnection between the present Guadalete River
324 channel and the former one (present San Pedro River channel), was made during the 18th century.

325 *5.2. Topographic mapping and multispectral image investigations (UAV devices)*

326 After processing the RGB and multispectral images, different photogrammetric and index maps were obtained.
327 NDVI index derived from the multispectral sensor reflects the phenological state of the plants, which is a
328 consequence of the infrared radiation being more strongly reflected in comparison to the visible part of the
329 electromagnetic spectrum. So, for the same vegetal species, wheat in this case, differences in the NDVI cannot
330 be related to interspecific variation but to subtle differences in plant vigour. These could be related to changes
331 in soil composition, but, in our case, they must be related to differences in porosity and permeability due to
332 the presence of hidden structures. These hidden structures have the clear pattern of a human settlement and are
333 evident in Figure 5.

334 Furthermore, in the RGB orthomosaic, these structures are also evident which point out to a surface expression
335 of them due to both subtle topographic differences and changes in wheat density and vigour (Figure 6). These
336 results also indicate the hidden structures must be at a very low depth because, although depending on soil
337 structure and composition, 70% of the wheat roots are normally at depths of less than 50 cm, and 50% being
338 at less than 25 cm (King et al., 2001). The results show a clear urban structure partly buried under the present
339 soil: La Martela settlement (see Figure 12). The structure is closed by a perimeter wall where some bastions
340 can be even identified. The urban structure is surrounded by darker areas, which in its northern side take the
341 form of an E-W channel about 30 m wide. The channel is limited to the North by a shallow structure with ramp
342 morphology. Inside the main urban structure, a set of parallel lines NNE-SSW oriented can be distinguished
343 and interpreted as streets (Figure 6, right).

344 *5.3. Geophysical GPR research*

345 Into La Martela archaeological site, we detected the first layer of materials up to 30 cm deep, without structures
346 and with different lines, which we could call as layers, very close together and corresponding to the soil moved
347 at the surface for farming activities. A second layer is where the structures were found at a depth of 40 cm,
348 with a wave propagation speed of 11.60 cm/ns. The walls measured between 25 and 45 cm (Figure 7). In some
349 cases, these structures were detected in noise level up to -1 m. The total detection depth was approximately 1

m, from which we only obtained noise. This may be due to the type of soil or the proximity of rigid geological levels. However, in the peripheral areas of the whole site, three different layers were detected, especially in the south and west of the site, corresponding with the ancient river bed. The first two levels corresponded largely to the first level of agricultural use, while the second one to archaeological structures. The third one, which was not detected in all areas of the exploration, appeared between 0.8 and 1.2 meters deep and may correspond to the bed level of the ancient coast.

5.4. Analysis from Cores

The sedimentological analysis of the cores included in this study reflects the main geomorphological elements present in the Bay of Cádiz, i.e. salt marshes, fluvial floodplain, dunes and beaches. Two key areas were identified for coring to address the objectives of this study: the Valdelagrana spit-barrier and its back area formed by the salt marshes system within the inner side of the Bay. A synthetic distribution of facies and depths of all the cores included in the present study can be seen in Figures 8, 9 and 10.

5.4.1. Valdelagrana Spit (S2, S3, S4)

In this area three different boreholes were carried out by Alonso et al. (2015), N-S aligned.

- S2: The core site is located in the area of the progradation unit H4, in the southernmost area of Valdelagrana spit and is 9.5 m long. In the borehole, the water table was at 1 m depth and only a sedimentary unit (U1) was identified (Table 1). While the base of U1 is characterized by sandy facies almost devoid of organisms, the upper part showed an abundance of macro-fauna remains, primarily shells. The base of the boreholes was detected at cal. 745 a BP (Figure 8).
- S3: The core site is located on a N-S oriented sand bar of the unit H4. The sediment record is 6.5 m long and the water table was found at 2 m depth. In its stratigraphic sequence, the sedimentary unit U1 (Figure 8) is marked by the alternation of three different sandy finning-upward facies with bivalve shells (Table 1).
- S4: The sedimentary sequence is 5 m long and is located in the inner sand bar of the oldest unit H2. The water table appeared at 2.2 m depth and the observation of the stratigraphy led to the identification of 2 sedimentary units (Figure 8 and Table 1). The first one (U2, upper 2.4 m), represents a washover fan deposit, characterised by coarse sands plenty of mollusc bioclasts. The second unit (U3) is mostly constituted by clays, with a major content of organic matter and remains of macrofauna, and interpreted by Alonso et al. (2015) as a typical saltmarsh deposit. The ^{14}C calibrated dating carried out at the top and the base of U3 showed ages of cal. 1.88 and 2.8 ka BP, respectively. If we consider a constant sedimentation rate for unit U2, an average sedimentation rate of 1.7 mm/yr is obtained, and the base would correspond to an age of 3.37 ka BP.

The boreholes S2, S3 and S4, carried out in the eastern side of the Bay, record the formation of the Holocene beach ridges of Valdelagrana system. In particular, S4 shows a transition from tidal flat to active saltmarsh, indicating a progressive sedimentary infilling between 2.8 and 1.9 ka BP (Punic and Roman epochs) and during the development of the beach ridges H2 and H3. Here, the saltmarshes developed in the restricted area sheltered

by H2 ridge (Bronze-Phoenician age) and were covered by beach and dune levels, probably related to several wave-energetic events recorded in the zone and dated in 1.9 ka BP (Schneider et al., 2010; Rodríguez Vidal et al., 2011; Alonso et al., 2015). These events could justify the transition to beach sands (washover deposit) and the subsequent development of dune deposits. The presence of clays in the borehole S4, not recorded in S3 and S2, further demonstrated that the cores belong to different stages of evolution of Valdelagrana Spit.

5.4.2. Tidal Estuary system (S1, S5, S6, S7, S8)

The inner part of the Bay, located in the back area of Valdelagrana Spit, is characterized by a tidal plain environment. In this area, five different boreholes were carried out in W-SE direction.

- S1: This core was also included in the study made by Alonso et al. (2015). With a maximum depth of 6.5 m, it was performed in an area of tidal plain inside a palaeomeander of the ancient Guadalete River and is composed of three different sedimentary units (Figure 9 and Table 2). The lower unit (U4) is characterized by sandy facies interpreted as a remnant of the historical beach ridge H3. The upper sedimentary units (V1, U3), made of muddy sands and clays, testify the transition from an estuarine environment to a salt marsh system. Radiocarbon dating of samples taken in the U4 unit gave an age between cal. 2.5 and 2.86 ka BP.
- S5: The core is located in the tidal plain developed to the south of San Pedro tidal channel and reaches a maximum depth of 6 m. The water table was detected at 0.6 m depth. Three different sedimentary units were identified (Table 2) and, in particular, the saltmarsh deposits (U3) are coeval to the development of the beach ridge H2. In this case, the deposition of sediments is characterized by a cyclic sequence with the alternation of muddy and sandy facies (Figure 9). The stratigraphic succession is similar to the one of core S1, but in S5 clay deposits show an alternation between saltmarsh levels and tidal channel facies, ending with dried-up saltmarshes in the upper 1.7 m. An isolated sand level with plenty of bioclasts is recorded between 1.1 and 1.7 m, which could be the sedimentary consequence of a very recent energetic event, like the tsunami that affected the bay in 1755. Between the three samples taken for radiocarbon dating, just one returned a reliable value and dated the base of the unit U4 (Table 3, sample S5_a1) at cal. 3.1 ka cal. BP.
- S6: The core is located inside the saltmarshes system in the back area of Valdelagrana spit and reaches a maximum depth of 8 m. The water table was detected at 1.2 m below the surface and three different sedimentary units were identified (Figure 10 and Table 2). While units V1 and U3 are made of muds rich in organic matter, typical of a saltmarsh environment, unit U4 is characterized by an increasing grain-size sequence rich in rounded clasts and reflecting a depositional environment with higher energy. From a clear fluvial environment at - 7 m a progressive transition is made to tidal channel facies, then to typical active saltmarsh deposits, and the core ends with dried-up saltmarshes in the upper 1.3 m. In this borehole, no samples were collected for radiocarbon dating and, consequently, the stratigraphic sequence was correlated to S7 and S8 cores.

- S7: The core, performed in the same area as the previous one, has a maximum depth of 9.5 m and along its stratigraphic succession three sedimentary units were detected (Figure 10 and Table 2). The content of organisms, mainly gastropods, decreases with depth, maybe due to different salinity levels. A carbonate level develops at a depth of 730 cm. This core repeats the sequence recorded in S6, with a transition at -7.9 m from tidal channel with fluvial influence to tidal channel and then to saltmarshes. This last transition took place around 7.0 ka BP, as proved by the collected sample for radiocarbon dating S7_a1, coeval with beach ridge H1 (although not recorded in the bay of Cadiz).
- S8: The core is located in the SE area of the saltmarshes characterizing the external bay and has a maximum depth of 7.5 m. Four different sedimentary units were identified (Figure 10 and Table 2) with a decreasing grain-size and abundance of macro-fauna remains from the base to the top. While the first sedimentary unit V1 is made of clays with no organisms, U5 consists entirely of a marine shells deposit. The transition from marine environment (U5) to tidal channel (U4) was recorded between 7.1 and 7.3 ka BP, during the Flandrian eustatic maximum and right before the development of H1 ridge. The core is completed by a typical transition from tidal environment (U4) to dried-up saltmarsh (V1, upper 1.3 m), by way of active saltmarshes environments (U3).

The boreholes S6, S7 and S8 reach the oldest deposits studied so far and dated at about 6.7 ka BP, when the Flandrian Transgression reached its maximum level in the Bay of Cádiz. The correlation between S7 and S8 sets the development of the marsh environment around 6.5 ka BP and the oldest deposits are made of beach sands with fluvial influence moving south-eastwards. Probably, around 6.5 ka BP the coastline reached this area, influenced also by the morphology of the Guadelete River estuary. The formation of the sand bars of Valdelagrana favoured the sedimentary infilling of the area turning it into the oldest salt marshes of the sector, with a sedimentation rate of 0.7 mm/y.

5.4.3. Radiocarbon dating and sedimentation rates

Datings from boreholes S1 (samples taken at 6 and 4.8 m depth), S2 (sample taken at 9.5 m depth) and S4 (samples taken at 4.0 and 2.5 m depth) were obtained from Alonso et al. (2015) and recalibrated by using up-to-date calibration curves and taking into account the Gulf of Cádiz reservoir effect, as explained in the Methodology section. The rest of the dating included in Table 3 are unpublished.

The calculation of average sedimentation rates, obtained by simply dividing sample depth and radiocarbon age, involves a number of errors that were not taken into account: dating errors linked to the ^{14}C radiocarbon procedure and reservoir effect; presence of interbedded sand and clay layers in the boreholes which present very different geomechanical properties, and natural processes of saltmarsh clay compaction (by sedimentary deflocculation, dehydration, physico-chemical processes related to early diagenesis, among others). All these sources of errors make us consider results as merely indicative, intending to understand how the geographic location of boreholes could have affected sedimentation. For the saltmarshes located in the northern Bay of Cádiz, boreholes S7 and S8 gave sedimentation rate values of 0.71 and 0.83 mm/yr, respectively. Boreholes

446 located near San Pedro tidal creek, S1, S4 and S5, gave moderate values, of 2.38 and 1.7 mm/yr respectively,
447 probably related to the sediment supply associated with the dynamics of the tidal channel.

448

449 **6. Discussion**

450 Considering all data exposed in the present work and correlating them to previous researches carried out in the
451 study area (Rodríguez Ramírez et al., 1996; Dabrio et al., 2000; Alonso et al., 2014; 2015; Rodríguez Vidal et
452 al., 2014), four morpho-evolutive scenarios (Figure 11) of the Northern Bay of Cádiz have been proposed,
453 respectively related to 6.5 ka BP, 3.0 ka BP, 2.0 ka BP and the present-day morphology of the area.

454 After the Holocene eustatic highstand about 6.5 ka BP (Figure 11a), the relative sea level was affected by a
455 slight fall followed by a later still-stand (Dabrio et al., 2000; Borja, 2013). During this period, as testified by
456 the stratigraphic succession of the boreholes, a first saltmarsh formed in an initial wide embayment located in
457 the NE zone, controlled by faults and mainly affected by tides. The embayment recorded a vertical sedimentary
458 infilling and the generation of saltmarshes and tidal channels in the central and inner zones.

459 Around 3.0 ka BP the study area was affected by an additional slight relative sea-level fall, as a consequence
460 of climate cooling (Issar, 2003; Borja, 2013), although other authors considered that by ca. 4.0 ka BP the fluvial
461 input to the bay surpassed the already negligible rate of sea-level rise, causing partial emergence of tidal flats
462 and spit barriers in this largely filled estuary (Dabrio et al., 2000). Regardless of the exact behaviour of sea
463 level at the bay, not known to such detail, this situation favoured the generation of beach ridge H2 (Figure
464 11b), active until Punic period (4.2-2.6 ka BP, Alonso et al., 2014; 2015). Within the Bay, the tidal influence
465 appeared to be more restricted, as testified by the stratigraphic succession of the borehole S5, and important
466 changes in the normal circulation of water through the channels used by Phoenicians for navigation took place.
467 Those changes can be related to two different causes. In the first instance, they can be ascribable to the above-
468 mentioned sea-level fall, which would have caused a depth decrease in the channels and their abandonment.
469 The second cause can be related to a high energy event, probably a tsunami, that was recorded in the study
470 area around 2.7-2.3 ka BP and which produced the breaching of Holocene littoral ridges at Valdelagrana
471 (Gracia et al., 2005) and other places along the coast of the Gulf of Cádiz, like Doñana (Rodríguez Vidal et
472 al., 2014).

473 With the increasing fluvial influence, a part of the Phoenician colony of Doña Blanca was probably moved to
474 a sandy island located to the north of the Guadalete River channel (Figure 12). In particular, the analysis of
475 those data allowed reconstructing a palaeogeographic scenario, which led to hypothesize the presence of a
476 fluvial harbour connected with the main settlement northernmost located. It is worthy to note that several
477 previous studies assumed the presence of a port facility in the area by that time (Ruiz Mata, 1999a; 1999b) but
478 the multidisciplinary analysis presented in this work, by means of overlapping stratigraphic data, the georadar
479 survey, and the multispectral image investigations, enabled its identification and classification.

Indeed, the location of Doña Blanca ancient city suggests the presence of a substratum adequate for the funding of buildings and walls. The almost exclusive clayey nature of the surface sediments along the Northern Bay of Cádiz prevent any possible urban settlement, which in fact is absent along the saltmarshes covering all this wide space. As a consequence, it can be deduced the existence of another kind of sediments under the ancient city, very probably richer in sand fraction. Perhaps this archaeological settlement indirectly indicates the presence of a sedimentary remain of an ancient fluvial island, as demonstrated by the structure detected through the georadar survey and the multispectral image investigations (Figures 5 and 6).

At the same time, in the study area, the sedimentary aggradation was going on, together with the fluvial flooding events, which led to hypothesize the presence of a fluvial harbour, perhaps connected with the main Doña Blanca settlement northernmost located, although this possible connection has not been proved yet. As demonstrated by the stratigraphic logs of cores S6, S7 and S8, during this period the tidal saltmarsh environment was completely developed in the whole inner and central zones of the Bay.

Around 2.0 ka BP (Figure 11c), the study area was characterized by a relative sea-level still-stand and an increase in fluvial sedimentary supplies due to massive deforestation and land clearing for wood exploitation (Alonso et al., 2009). In this period, the third-generation of beach ridge H3 formed (2.3-1.1 ka BP, Alonso et al., 2014; 2015) causing the restriction of tidal channels activities in the Northern Bay of Cádiz and the almost complete prevalence of fluvial processes (Figure 11c). In this framework of events, the artificial opening of a second fluvial channel connecting the Guadalete estuary with the sea at Puerto de Santa María has been included in Figure 11c, together with the initial development of salinas and salt harvesting exploitations through the main tidal channels along the whole Bay of Cádiz.

During the Little Ice Age, the global sea level was affected by a slight fall (Grinsted et al., 2010; Kemp et al., 2011), the end of which was identified by Marcos et al. (2011) in the Bay of Cádiz through the analysis of a historical tide gauge. We cannot discard an increase in the fluvial sediment supply to the bay due to intense deforestation carried out in Spain during the 19th century (Tomás y Valiente, 1978). All these factors favoured the formation of the youngest H4 beach ridge (1.0 ka BP, Alonso et al., 2014; 2015), detected within the stratigraphic successions of the boreholes S2 and S3. In addition, this period was characterized by the development and the subsequent abandonment of salt harvesting exploitations and by the complete disconnection of the San Pedro tidal channel from the Guadalete River.

In more recent times (Figure 11d), the vicinity of Doña Blanca settlement has been affected by a rapid lateral migration of the Guadalete River, burying the archaeological structure, as demonstrated by the geomorphological map of Figure 4, and by the documented wave energetic event (i.e. tsunami) in 1755.

Regarding sedimentation rates, values obtained in the present work are notably lower than those calculated in other zones of the Bay of Cadiz, using the same methodology. Data from the Iro River mouth, in the southern Bay, reach values of almost 10 mm/yr, while in the northern Bay no borehole records values higher than 2.5 mm/yr. Boreholes S7 and S8 show lower values than S1 and S5, suggesting a direct relationship between

sedimentation rates and proximity to natural sediment suppliers - e.g. river mouths. S7 and S8, located in the middle of the northern saltmarshes, record the lowest value in the whole Bay of Cádiz, also conditioned by their artificial desiccation during the middle 20th century.

The obtained results are comparable to other similar records in the Ría of Huelva saltmarshes, a sedimentary system located within the Gulf of Cádiz, with very similar geomorphological, tidal, climatic and fluvial characteristics. Morales et al. (2003) used mechanical boreholes to calculate sedimentation rates in the Huelva saltmarshes, obtaining values between 2.10 and 4.50 mm/yr in high, marginal marshes, and between 1.22 and 2.40 mm/yr at points located in high marshes close to the main fluvial channel. These values are perfectly comparable with those obtained in Valdelagrana boreholes, S1 and S5. The highest values were obtained in floodable northern Bay of Cádiz, between 0.71 and 0.83 mm/yr (boreholes S7 and S8), while in Huelva the greatest values, always related to low marshes, reach almost 10 mm/yr (Morales et al., 2003). As a conclusion, although the values of sedimentation rates obtained in the present study are merely orientative, results are lower but perfectly comparable to those obtained by other authors in nearby saltmarshes under roughly similar geomorphodynamic conditions.

7. Concluding remarks

The present research presents the reconstruction of the geomorphological evolution of the northern Bay of Cádiz since the mid-Holocene, not only by defining the ancient beach ridges located within the study area but also by characterizing the evolution of its depositional environments over time. A general transition is recorded between an initial wide embayment, fully controlled by marine processes, to a final alluvial plain, almost exclusively affected by fluvial processes.

The multidisciplinary study of the Bay and, in particular, of the Phoenician colony of Doña Blanca resulted in the modelling of four different palaeoenvironmental scenarios reconstructing the evolution of the study area between the last eustatic maximum, around 6.5 ka BP, and the present day. Contrary to what was hypothesized in the past, the scenarios here proposed show that the settlement of Doña Blanca was already located far away from the coastline and near the Guadalete River at the time of its construction. The study of the colony of Doña Blanca, carried out using stratigraphic data, georadar surveys, and multispectral and topographic image investigations, led to the reconstruction of another palaeogeographic scenario, representing the Phoenician settlement at the time of its construction and identifying for the first time the remains of a second settlement interpreted as a harbour area (La Martela settlement, Figure 12). Besides, the overlap between the UAV surveys and the stratigraphic reconstructions let us suppose that this was a fluvial harbour, due both to its inland position and the recognition of the depositional environments surrounding it. The slight relative sea-level fall during the Little Ice and the increase in the sediment supply to the bay due to regional deforestation favoured coastal progradation and the prevalence of fluvial processes with respect to tides in this area, which finally lead to the destruction of La Martela Punic harbour and its burial by fluvial sediments.

The high-resolution stratigraphic data allowed evaluating the average sedimentation rates of the study area. During the last 6.5 ka BP, the sedimentation rates increased over time allowing the formation of Valdelagrana Spit.

Author Contributions

C.Caporizzo: geomorphological and stratigraphic interpretations, conceptualization, methodology, software, writting, **F.J. Gracia**: geomorphological and stratigraphic interpretations, conceptualization, supervision, writting, **P.P.C. Aucelli, G. Mattei**: methodology, conceptualization, geomorphological and stratigraphic interpretations, supervision, **C.Martín-Puertas**: facies analysis, stratigraphy, sampling of cores, **L. Lagóstena, J.A. Ruiz**: georadar survey, archaeological support, interpretation, **C. Alonso, A. Higueras-Milena**: regional geoarchaeology, interpretation, **L. Barbero, J.A. López-Ramírez**: UAV surveys, interpretation, **I. Galán-Ruffoni**: reservoir effect correction on dating results.

Acknowledgements

Boreholes were funded by the Coastal Demarcation Service of Atlantic Andalusia in Cádiz (Spanish Ministry of the Environment). This is a contribution to the research group RNM-328 of the Andalusian Research Plan (PAI).

References

Alberico, I., Amato, V., Aucelli, P.P.C., Di Paola, G., Pappone, G., Rosskopf, C.M., 2012. Historical and recent changes of the Sele River coastal plain (Southern Italy): natural variations and human pressures. Rend. Lincei 23(1), 3-12.

Allen, J.R.L., 2000. Morphodynamics of Holocene salt marshes: a review sketch from the Atlantic and Southern North Sea coasts of Europe. Quat. Sci. Rev. 19, 1155-1231.

Alonso Millán, A., Pagés Valcarlos, J.L., 2010. Evolución del nivel del mar durante el Holoceno en el noroeste de la Península Ibérica. Rev. de la Soc. Geol. de España, 23 (3-4), 157-167.

Alonso, C., Gracia, F.J., 2004. La paleotopografía costera y el asentamiento de puertos, fondeaderos y zonas de producción del litoral gaditano durante la antigüedad. In: De Maria, L., Turchetti, R. (Eds.), Evolución paleoambiental de los puertos y fondeaderos antiguos en el Mediterráneo Occidental. Rubbettino, Roma, Italy, 167-195. I.S.B.N.: 88-498-1114-4.

Alonso, C., Gracia, F.J., Benavente, J., 2009. Evolución histórica del sector meridional de la Bahía Interna de Cádiz. RAMPAS 11, 13-37.

580 Alonso, C., Gracia, F., Rodríguez-Polo, S., 2014. Modelo de evolución histórica de la flecha-barrera de
581 Valdelagrana (Bahía de Cádiz). Geomorfología litoral: Procesos y Formas en las Costas, 584-587. XIII
582 Reunión Nacional de Geomorfologia, Cáceres, Spain.

583 Alonso, C., Gracia, F. J., Rodríguez-Polo, S., Martín-Puertas, C., 2015. El registro de eventos energéticos
584 marinos en la Bahía de Cadiz durante épocas históricas. In: Rodríguez-Vidal, J. (Ed.), Eventos energéticos
585 amarinos históricos y ocupación costera en el Golfo de Cadiz. Cuaternario & Geomorfología 29 (1–2), 95-117.

586 Amato, V., Aucelli, P.P.C., Cinque, A., D'Argenio, B., Di Donato, V., Papppne, G., Petrosino, P., Rosskopf,
587 C.M.; Russo Ermolli, E., 2011. Holocene palaeo-geographical evolution of the Sele river coastal plain
588 (Southern Italy): new morpho-sedimentary data from the Paestum area. Il Quaternario, 24, 5-7.

589 Amato, V., Aucelli, P.P.C., Mattei, G., Pennetta, M., Rizzo, A., Rosskopf, C.M., Schiattarella, M., 2018. A
590 geodatabase of Late Pleistocene-Holocene palaeo sea-level markers in the Gulf of Naples. Alpine Mediterr.
591 Quat. 31, 5-9.

592 Anthony, E., Marriner, N., Morhange, C., 2014. Human influence and the changing geomorphology of
593 Mediterranean deltas and coasts over the last 6000 years: From progradation to destruction phase? Earth-Sci.
594 Rev. 139, 336-361.

595 Aranda, M., Gracia, F.J., Peralta, G., 2020. Estuarine mapping and eco-geomorphological characterization for
596 potential application in conservation and management: three study cases along the Iberian coast. Appl. Sci.
597 10(3), 4429, doi:10.3390/app10134429.

598 Arteaga, O., D. Schulz, H., Roos, A., 2008. Geoarqueología Dialéctica en la Bahía de Cádiz. RAMPAS, 10,
599 21-116.

600 Ascione, A., Aucelli, P.P.C., Cinque, A., Di Paola, G., Mattei, G., Ruello, M., Russo Ermolli, E., Santangelo,
601 N., Valente, E., 2020. Geomorphology of Naples and the Campi Flegrei: human and natural landscapes in a
602 restless land. J. Maps, 1-11.

603 Aucelli, P.P.C., Cinque, A., Giordano, F., Mattei, G., 2016a. A Geoarchaeological Survey of the Marine
604 Extension of the Roman Archaeological Site Villa del Pezzolo, Vico Equense, on the Sorrento Peninsula, Italy.
605 Geoarchaeology, 31(3), 244-252. DOI: 10.1002/gea.21567

606 Aucelli, P.P.C., Cinque, A., Mattei, G., Pappone, G., 2016b. Historical sea level changes and effects on the
607 coasts of Sorrento Peninsula (Gulf of Naples): New constrains from recent geoarchaeological investigations.
608 Palaeogeogr. Palaeoclimatol. Palaeoecol. 463, 112-125.

609 Aucelli, P. P.C, Cinque, A., Mattei, G., Pappone, G., 2017. Late Holocene landscape evolution of the gulf of
610 Naples (Italy) inferred from geoarchaeological data. J. Maps 13(2), 300-310.

611 Aucelli, P. P.C., Cinque, A., Mattei, G., Pappone, G., & Stefanile, M. (2018a). First results on the coastal
612 changes related to local sea level variations along the Puteoli sector (Campi Flegrei, Italy) during the historical
613 times. Alpine Mediterr. Quat. 31, 13-16

614 Aucelli, P.P.C., Cinque, A., Mattei, G., Pappone, G., Stefanile, M., 2018b. Coastal landscape evolution of
615 Naples (Southern Italy) since the Roman period from archaeological and geomorphological data at Palazzo
616 degli Spiriti site. Quat. Int. 483, 23-38

617 Aucelli, P.P.C.; Cinque, A.; Mattei, G.; Pappone, G.; Stefanile, M., 2018c. First results on the coastal changes
618 related to local sea level variations along the Puteoli sector (Campi Flegrei, Italy) during the historical times.
619 Alpine Mediterr. Quat. 31, 13–16.

620 Aucelli, P.P.C., Cinque, A., Mattei, G., Pappone, G., Rizzo, A., 2019a. Studying relative sea level change and
621 correlative adaptation of coastal structures on submerged Roman time ruins nearby Naples (Southern Italy).
622 Quat. Int. 501, 328-348

623 Aucelli, P.P.C., Caporizzo, C., Cinque, A., Mattei, G., Pappone, G., Stefanile, M., 2019b. New insight on the
624 1st century BC paleo-sea level and related vertical ground movements along the Baia - Miseno coastal sector
625 (Campi Flegrei, southern Italy), Proceeding of 2019 IMEKO TC4 International Conference on Metrology for
626 Archaeology and Cultural Heritage, MetroArchaeo 2019, pp. 474-477.

627 Aucelli, P.P.C., Mattei, G., Caporizzo, C., Cinque, A., Troisi, S., Peluso, F., Stefanile, M., Pappone, G., 2020.
628 Ancient coastal changes due to ground movements and human interventions in the Roman Portus Julius
629 (Pozzuoli Gulf, Italy): Results from photogrammetric and direct surveys. Water 12(3), 658.

630 Auriemma, R., Solinas, E. 2009. Archaeological remains as sea level change markers: A review. Quat. Int.
631 206, 134-146, doi:10.1016/j.quaint.2008.11.012.

632 Bailey, G., Galanidou, N., Peeters, H., Jöns, H., Mennenga, M. (Eds.), 2020. The Archaeology of Europe's
633 Drowned Landscapes. Coastal research Library, 35. Springer Open, 560 pp.

634 Benavente, J., Gracia, F.J., López-Aguayo, F., 2000. Empirical model of morphodynamic beachface behaviour
635 for low-energy mesotidal environments. Mar. Geol. 167, 375-390.

636 Borja, F., Zazo, C., Dabrio, C.J., Díaz del Olmo, F., Goy, J.L., Lario, J., 1999. Holocene aeolian phases and
637 human settlements along the Atlantic coast of southern Spain. Holocene 9, 337-339.

638 Borja, F., 2013. La desembocadura del Guadalquivir en la segunda mitad del Holoceno. Síntesis
639 paleogeográfica. In: García, L., Vargas, J.M., Hurtado, V.; Ruiz, T., Cruz-Auñón, R. (Eds.), El asentamiento
640 prehistórico de Valencina de la Concepción (Sevilla), 93-112. Universidad de Sevilla, Sevilla, Spain.

641 Botto, M., 2014. Los fenicios en la Bahía de Cádiz. Nuevas investigaciones. In: Botto, M. (Ed) Collezione di
642 Studi Fenici, 46. Fabrizio Serra Editore, Pisa-Roma, Italy.

643 Burningham, H., Cooper, J.A.G., 2004. Morphology and historical evolution of north-east Atlantic coastal
644 deposits: the west Donegal estuaries, north-west Ireland. J. Coast. Res. SI 41, 148-159.

645 Cuven, S., Paris, R., Falvard, S., Miot-Noirault, E., Benbakkar, M.; Schneider, J.L.; Billy, I. (2013). High-
646 resolution analysis of a tsunami deposit: Case-study from the 1755 Lisbon tsunami in southwestern Spain.
647 Mar. Geol. 337, 98-111.

648 Dabrio, C.J., Zazo, C., Goy, J.L., Sierro, F.J., Borja, F., Lario, J., González, J.A., Flores, J.A., 2000.
649 Depositional history of estuary infill during the last postglacial transgression (Gulf of Cadiz, Southern Spain).
650 Mar. Geol. 162, 381-404.

651 Degeai, J. P., Bertoncello, F., Vacchi, M., Augustin, L., de Moya, A., Ardito, L., Devillers, B., 2020. A new
652 interpolation method to measure delta evolution and sediment flux: Application to the late Holocene coastal
653 plain of the Argens River in the western Mediterranean. Mar. Geol. 106159.

654 Del Río, L., Benavente, J., Gracia, F.J., Alonso, C., Rodríguez Polo, S., 2015. Anthropogenic influence on spit
655 dynamics at various timescales: Case study in the Bay of Cadiz (Spain). In: Randazzo, G., Jackson, D.W.,
656 Cooper, J.A.G. (Eds.), Sand and Gravel Spits. Coastal Research Library 12, Springer, Dordrecht, Netherlands,
657 123-138.

658 Del Río, L., Benavente, J., Gracia, F. J., Anfuso, G., Aranda, M., Montes, J.B., Puig, M., Talavera, L.,
659 Plomaritis, T.A., 2019. Beaches of Cadiz: Dynamic Processes, Sediments and Management. Springer, Cham.
660 http://doi-org-443.webvpn.fjmu.edu.cn/10.1007/978-3-319-93169-2_14.

661 Edwards, R.J., Horton, B.P., 2000. Reconstructing relative sea-level change using UK saltmarsh foraminifera.
662 Mar. Geol. 169, 41-56.

663 Eleveld, M., 2015. The Application of Airborne Laser Scanning Systems in Archaeology: Moving beyond
664 pretty pictures. M. Bekkema, UNIGIS Mod. 6, Vrije Universiteit, Amsterdam, 14 pp.

665 Fa, D., Lario, J., Smith, P., Finlayson, J.C., 2000. Elementos sumergidos kársticos alrededor de la costa de
666 Gibraltar y su potencial uso por humanos en la Prehistoria. In: Santiago, P., Martínez, A., Mayoral, J. (Eds.),
667 Actas I Congreso Andaluz de Espeleología, Federación Andaluza de Espeleología, pp. 143-149.

668 Fernández-Hernández, J., González-Aguilera, D., Rodríguez-Gonzálvez, P., Mancera-Taboada, J., 2015.
669 Image-Based Modelling from Unmanned Aerial Vehicle (UAV) Photogrammetry: An Effective, Low-Cost
670 Tool for Archaeology Applications. Archaeometry 57 (1), 128-145.

671 Fernández-Montblanc, T., Izquierdo, A., Bethencourt, M., 2014. Underwater cultural heritage risk assessment
672 related to mean and extreme storm events: A modelling case study in the Bay of Cadiz. In: Candelera, R. (Ed.),
673 Science, Technology and Cultural Heritage. Taylor & Francis Group, London, pp. 83-88.

674 García de Domingo, J., González, J., Hernáiz, P.P., 1987. Memoria y mapa geológico E/1:50000 de la hoja
675 1068 (San Fernando). Instituto Geológico y Minero de España, Madrid.

676 Giaime, M., Marriner, N., Morhange, C., 2019. Evolution of ancient harbours in deltaic contexts: A
677 geoarchaeological typology. Earth-Sci. Rev. 191, 141-167.

678 Gracia, F.J., Rodríguez-Vidal, J., Benavente, J., Cáceres, L., López-Aguayo, F., 1999. Tectónica cuaternaria
679 en la Bahía de Cadiz. In: Pallí, L., Roqué, C. (Eds.), Avances en el estudio del Cuaternario español. University
680 of Girona, Spain, pp. 67-74.

681 Gracia, F.J., Alonso, C., Anfuso, G., Benavente, J., Del Río, L., Domínguez, L., Martínez, J.A., 2005. Chapter
682 IV: Historical evolution and erosion problems in the Cádiz Coast. En: Geomorphology of the South-Atlantic
683 Spanish Coast (F.J. Gracia, Coord.). 6th Int. Conf. on Geomorphology, Field trip guide A-4. Zaragoza, 40-58.

684 Gracia, F.J., Rodríguez-Vidal, J., Belluomini, G., Cáceres, L. M., Benavente, J., Alonso, C., 2008. Diapiric
685 uplift of an MIS 3 marine deposit in SW Spain. Implications in Late Pleistocene sea level reconstruction and
686 palaeogeography of the Strait of Gibraltar. Quat. Sci. Rev. 27(23-24), 2219-2231.

687 Gracia, F.J., Martín, C., 2009. Realización y datación de sondeos en la bahía de Cádiz y las marismas del
688 Barbate. Ministerio de Medio Ambiente y Medio Rural y Marino, 116 pp.

689 Gracia, F.J., Alonso, C., Abarca, J.M., 2017. Evolución histórica y geomorfología de las explotaciones
690 salineras en marismas mareales. Ejemplos de la bahía de Cádiz. Cuaternario y Geomorfología 31 (1-2), 45-72.

691 Grinsted, A., Moore, J.C., Jevrejeva, S., 2010. Reconstructing sea level from paleo and projected temperatures
692 200 to 2100 AD. Climate Dynamics, 34, 461-472.

693 Gutiérrez-Mas, J.M., Achab, M., Gracia, F.J., 2004. Structural and physiographic controls on the Holocene
694 marine sedimentation in the Bay of Cadiz (SW Spain). Geodin. Acta 17 (2), 47-55.

695 Gutiérrez-Mas, J.M., 2011. Glycymeris shell accumulations as indicators of recent sea-level changes and high-
696 energy events in Cádiz Bay (SW Spain). Estuar. Coast. Shelf Sci. 92, 546-554.

697 Gutiérrez-Mas, J.M., López-Arroyo, J., Morales, J.A., 2009. Recent marine lithofacies in Cadiz Bay (SW
698 Spain). Sequences, processes and control factors. Sediment. Geol. 218, 31-47.

699 Issar, A.S., 2003. Climate changes during the Holocene and their impact on hydrological systems. Cambridge
700 University Press, Cambridge, United Kingdom, 144 pp.

701 Kemp, A.C., Horton, B.P., Donnelly, J.P., Mann, M.E., Vermeer, M., Rahmstorf, S., 2011. Climate related
702 sea-level variations over the past two millennia. PNAS 108 (27), 11017-11022.

703 Khan, N.S., Horton, B.P., Engelhart, S., Rovere, A., Vacchi, M., Ashe, E.L., Törnqvist, T.E., Dutton, A.,
704 Hijma, M.P., Shennan, I., 2019. Inception of a global atlas of sea levels since the Last Glacial Maximum. Quat.
705 Sci. Rev. 220, 359-371.

King, J., Gay, A., Sylvester-Bradley, R., Bingham, I., Foulkes, J., Gregory, P. and Robinson, D., 2001. Modelling Cereal Root Systems for Water and Nitrogen Capture: Towards and Economic Optimum. Ann. Bot. 91, 383-390.

Koster, B., Reicherter, K., 2014. Sedimentological and geophysical properties of a ca. 4000 year old tsunami deposit in southern Spain. Sedimen. Geol. 314, 1-16.

Lambeck, K., Antonioli, F., Anzidei, M., Ferranti, L. Leoni, G., Scicchitano, G., S. Silenzi, S., 2011. Sea level change along the Italian coast during the Holocene and projections for the future. Quat. Int.232, 250-257, doi:10.1016/j.quaint.2010.04.026.

Lario, J., Luque, L., Zazo, C., Goy, J.L., Spencer, C., Cabero, A., Bardají, T., Borja, F., Dabrio, C.J., Civis, J., González-Delgado, J., Borja, C., Alonso-Azcárate, J., 2010. Tsunami vs. storm surge deposits: a review of the sedimentological and geomorphological records of extreme wave events (EWE) during the Holocene in the Gulf of Cadiz, Spain. Zeitschrift für Geomorphol. 54 (3), 301-316.

Leorri, E., Gehrels, W.R., Horton, B.P., Fatela, F. and Cearreta, A. 2010. Distribution of foraminifera in salt marshes along the Atlantic coast of SW Europe: Tools to reconstruct past sea-level variations. Quat. Int. 221, 104–115, doi:10.1016/j.quaint.2009.10.033.

Lagóstena Barrios, L., Ruiz Gil, J.A., Pérez Marrero, J., Trapero Fernández, P., Catalán González, J. Martín Mochales, Parrilla Giráldez, R.., Rondán Sevilla, I., Ruiz Barroso, M., 2020. GPR survey and methods in archaeological visualization: the punic harbour of La Martela (El Puerto de Santa María, Spain) as case study. Geophysics (in press).

Lagóstena Barrios, L., Ruiz Gil, J.A., 2020. El puerto romano de Gades: nuevos descubrimientos y noticias sobre sus antecedentes. Il Mediterraneo e la Storia III. Documentando città portuali. Capri. Acta Instituti Romani Finlandiae (in press).

Madden, M., Jordan, T., Bernardes, S., Cotten, D., O'Hare, N., Pasqua, A., 2015. Unmanned Aerial Systems (UAS) and Structure from Motion (SfM) Revolutionize Wetlands Mapping. In: Tiner, R., Lang, M., Klemas, V. (Eds.), Remote Sensing of Wetlands: Applications and Advances, CRC Press Taylor & Francis Group, Boca Raton, Florida, U.S.A, 10, 195-222.

Mann, T., Bender, M., Lorscheid, T., Stocchi, P., Vacchi, M., Switzer, A., Rovere, A., 2019. Relative sea-level data from the SEAMIS database compared to ICE-5G model predictions of glacial isostatic adjustment. Data Brief 27, 104600.

Marcos, M., Puyol, B., Wöpperlmann, G., Herrero, C., García-Fernández, M.J., 2011. The long sea level record at Cadiz (southern Spain) from 1880 to 2009. J. Geophys. Res. 116 (C12003), 1-10.

Marriner, N., Morhange, C., 2007. Geoscience of ancient Mediterranean harbours. Earth-Sci. Rev. 80, 137-194.

739 Martins, J.M.M.; Soares, A.M.M., 2013. Marine Radiocarbon Reservoir Effect in Southern Atlantic Iberian
740 Coast. Radiocarbon 55 (2-3), 1123-1134.

741 Mattei, G., Troisi, S., Aucelli, P. P., Pappone, G., Peluso, F., & Stefanile, M., 2018a. Multiscale reconstruction
742 of natural and archaeological underwater landscape by optical and acoustic sensors. In 2018 IEEE International
743 Workshop on Metrology for the Sea; Learning to Measure Sea Health Parameters (MetroSea) (pp. 46-49).
744 IEEE.

745 Mattei, G., Troisi, S., Aucelli, P. P., Pappone, G., Peluso, F., Stefanile, M., 2018b. Sensing the submerged
746 landscape of Nisida Roman Harbour in the Gulf of Naples from integrated measurements on a USV. Water
747 10(11), 1686.

748 Mattei, G., Rizzo, A., Anfuso, G., Aucelli, P. P. C., Gracia, F.J., 2019. A tool for evaluating the archaeological
749 heritage vulnerability to coastal processes: The case study of Naples Gulf (southern Italy). Ocean & Coastal
750 Management 179, 104876.

751 Morales, J.A., San Miguel, E.G., y Borrego, J., 2003. Tasas de sedimentación reciente en la Ría de Huelva.
752 Geogaceta 33, 15-18.

753 Morhange, C. (Ed.), 2000. Ports antiques et paléoenvironnements littoraux. Mediterranée, 94(1.2), 111 pp.

754 Morhange, C., Marriner, N., Excoffon, P., Bonnet, S., Flaux, C., Zibrowius, H., Goiran, J.P., El Amouri, M.,
755 2013. Relative sea-level changes during Roman times in the Northwest Mediterranean: The 1st Century A.D.
756 fish tank of Forum Julii, Fréjus, France. Geoarchaeology 28, 363-372.

757 Niveau de Villedary, A. M., Ruiz Mata, D., 1995. El poblado de Las Cumbres (Castillo de Doña Blanca).
758 Urbanismo y materiales del siglo III a.C. Actas del IV Congreso internacional de estudios fenicios y púnicos,
759 Cádiz, Spain, 2-6 octubre, 893-903.

760 Niveau de Villedary, A.M., 2019. La etapa arcaica de la ciudad fenicia de Gadir. Lucentum 38, 111-138.

761 Pachón Veira, R. F., Manzano Agugliaro, F., 2005. Interpretación 3D del barrio fenicio de Doña Blanca (Puerto
762 de Santa Maria, Cádiz). Actas del XVII Congreso Internacional de Ingeniería gráfica. Edición electrónica.
763 Sevilla, Spain, Junio.

764 Pappone, G., Aucelli, P. P. C., Aberico, I., Amato, V., Antonioli, F., Cesarano, M., Di Paola, G., Pelosi, N.,
765 2012. Relative sea-level rise and marine erosion and inundation in the Sele river coastal plain (Southern Italy):
766 scenarios for the next century. Rend. Lincei 23(1), 121-129.

767 Pappone, G., Aucelli, P. P., Mattei, G., Peluso, F., Stefanile, M., Carola, A., 2019. A Detailed Reconstruction
768 of the Roman Landscape and the Submerged Archaeological Structure at “Castel dell’Ovo islet” (Naples,
769 Southern Italy). Geosciences 9(4), 170.

770 Passchier, C.W., Wiplinger, G., Güngör, T., Kessener, P., Sürmelihindi, G., 2013. Normal fault displacement
771 dislocating a Roman aqueduct of Ephesos, western Turkey. Terra Nova 25(4), 292-297.

772 Pérez Fernández, E., 2018. Las intervenciones antrópicas en el curso bajo del Guadalete y el San Pedro durante
773 la Edad Moderna. Riparia 4, 146-190.

774 Rahman, R., Plater, A.J., 2014. Particle-size evidence of estuary evolution: A rapid and diagnostic tool for
775 determining the nature of recent saltmarsh accretion. Geomorphology 213, 139-152.

776 Reimer, P.J., Bard, E., Bayliss, A., Beck, J.W., Blackwell, P.G., Bronk Ramsey, C., Buck, C.E., Cheng, H.,
777 Edwards, R.L., Friedrich, M., Grootes, P.M., Guilderson, T.P., Haflidason, H., Hajdas, I., Hatté, C., Heaton,
778 T.J., Hoffmann, D.L., Hogg, A.G., Hughen, K.A., Kaiser, K.F., Kromer, B., Manning, S.W., Niu, M., Reimer,
779 R.W., Richards, D.A., Scott, E.M., Southon, J.R., Staff, R.A., Turney, C.S.M., van der Plicht, J., 2013.
780 IntCal13 and Marine13 Radiocarbon Age Calibration Curves, 0-50,000 Years cal BP. Radiocarbon 55(4),
781 1869–1887.

782 Rodríguez-Polo, S., Gracia, F.J., Benavente, J., Del Río, L., 2009. Geometry and recent evolution of the
783 Holocene beach ridges of the Valdelagrana littoral spit (Cádiz Bay, SW Spain). J. Coast. Res. S.I. 56, 20-23.

784 Rodríguez-Ramírez, A., Rodríguez Vidal, J., Cáceres, L., Clemente, L., Belluomini, G., Manfra, I., Improta,
785 S., De Andrés, J.R., 1996. Recent coastal evolution of the Doñana national park (SW Spain). Quat. Sci. Rev.
786 15, 803-809.

787 Rodríguez-Vidal, J., Ruiz, F., Cáceres, L.M., Abad, M., González-Regalado, M.L., Pozo, M., Carretero, M.I.,
788 Monge, A.M., Gómez-Toscano, F., 2011. Geomarkers of the 218-209 BC Atlantic tsunami in the Roman Lacus
789 Ligustinus (SW Spain): a palaegeographical approach. Quat. Int. 242, 201-212.

790 Rodríguez-Vidal, J., Bardají, T., Zazo, C., Goy, J.L., Borja, F., Dabrio, C.J., Lario, J., Cáceres, L.M., Ruiz, F.,
791 Abad, M., 2014. Coastal dunes and marshes in Doñana National Park. In: Gutiérrez, F., Gutiérrez, M. (Eds),
792 Landscapes and Landforms of Spain. World Geomorphological Landscapes Series. Springer, Dordrecht,
793 Netherlands, 229-238.

794 Ruiz, J. A., Lagóstena, L., Pérez, J., Trapero, P., Catalán, J., Martín, D., Parrilla, R., Rondán, I., 2020. The
795 Phoenician site of Castillo de Doña Blanca, geophysics and modeling contributions to its archaeological plan.
796 Archaeological Prospection (in press).

797 Ruiz Mata, D., Pérez, C.J., 1995. El poblado fenicio del Castillo de Doña Blanca. Revista de Historia de El
798 Puerto 15, 123-125.

799 Ruiz Mata, D., Niveau de Villedary, A. M., Vallejo Sánchez, M.J.I., 1998. La ciudad Tartésica-Turdetana.
800 Congreso Internaciónal -Los Iberos, Príncipes de Occidente -Sección 1.

Ruiz Mata, D., 1999a. The Phoenicians of the Archaic Epoch (8th-7th centuries B.C) in the bay of Cádiz (Spain). Cádiz and Castillo de Doña Blanca. Isimu: Revista sobre Oriente Próximo y Egipto en la antigüedad 2, 469-508

Ruiz Mata, D., 1999b. La fundación de Gadir y el Castillo de Doña Blanca. Contrastación textual y arqueológica *Complutum*. ISSN 1131-6993, ISSN-e 1988-2327, 10, 279-317.

Ruiz Mata, D., Vallejo Sánchez, J.I., Gómez González, J.I., Niveau de Villedary, A.M., 2005. El Centro de Estudios Protohistóricos Castillo de Doña Blanca. Atti del V Congresso Internazionale di Studi Fenici e Punici (Palermo-Marsala, 2-8 Ottobre 2000), vol. III.Università degli Studi di Palermo, Italy, 1153-1160.

Ruiz Mata, D, 2018. Varios aspectos sobre el vino y la bodega turdetana-púnica de la sierra de San Cristóbal, en El Puerto de Santa María (Cádiz). Revista de Historia de El Puerto 60, 9-131.

Sander, L., Hede, M.U., Fruergaard, M., Nielsen, L., Clemmensen, L.B., Kroon, A., Johnnessen, P.N., Nielsen, L.H., Pejrup, M., 2016. Coastal lagoons and beach ridges as complementary sedimentary archives for the reconstruction of Holocene relative sea-level changes. Terra Nova 28, 43-49.

Schneider, H., Höfer, D., Trog, C., Busch, S., Schneider, M., Baade, J., Daut, G. y Maüsbacher, R., 2010). Holocene estuary development in the Algarve Region (Southern Portugal) – A reconstruction of sedimentological and ecological evolution. Quat. Int. 221, 141-158.

Schulz, H.D., 1983. Zur lage Holozäner Küsten in den Mündungsgebieten des río de Vélez und des río Algarrobo (Málaga). Madrider Mitteilungen 24, 59-64.

Snavely, N., Seitz, S.M. and Szeliski, R., 2008. Modelling the world from internet photo collections. Int. J. Comput. Vis. 80 (12), 189-210.

Soares, A.M.M., Martins, M.M., 2009. Radiocarbon dating of marine shell samples. The marine radiocarbon reservoir effect of coastal waters off Atlantic Iberia during Late Neolithic and Chalcolithic Periods. J. of Archaeol. Sci. 36(12), 2875-2881.

Soares, A.M.M., 2015. Datación radiocarbónica de conchas marinas en el golfo de Cádiz: El efecto reservorio marino, su variabilidad durante el Holoceno e inferencias paleoambientales. Cuaternario y Geomorfología 29(1-2), 19-29.

Stuiver, M., Reimer, P., 2018. Extended 14C data base and revised CALIB 3.0 14C calibration program. Radiocarbon 35, 231-237.

Tomás y Valiente, F., 1978. El proceso de desamortización de la tierra en España. Agricultura y Sociedad 7, 11-33.

Vacchi, M., Rovere, A., Chatzipetros, A., Zouros, N., Firpo, M., 2014. An updated database of Holocene relative sea level changes in NE Aegean Sea. Quat. Int. 328-329, 301-310.

833 Vacchi, M., Marriner, N., Morhange, C., Spada, G., Fontana, A., Rovere, A., 2016. Multiproxy assessment of
834 Holocene relative sea-level changes in the western Mediterranean: Sea-level variability and improvements in
835 the definition of the isostatic signal. Earth-science reviews, 155, 172-197.

836 Vijande, E., Domínguez-Bella, S., Duarte, J., Martínez-López, J., Barrena-Tocino, A., 2015. Social inequalities
837 in the Neolithic of southern Europe: The grave goods of the Campo de Hockey necropolis (San Fernando,
838 Cádiz, Spain). CR Palevol 14, 147-161.

839 Westoby, M. J., Brasington, J., Glasser, N. F., Hambrey, M. J, and Reynolds, J. M., 2012. 'Structure-from-
840 Motion' photogrammetry: A low-cost, effective tool for geoscience applications. Geomorphology 179, 300-
841 314.

842 Zamora, J.A., Sáez, A.M., 2014. The oceanfront of Phoenician Cádiz: A new epigraphic find and its
843 palaeogeographic context. In: Botto, M., (Ed.), Los fenicios en la bahía de Cádiz, nuevas investigaciones.
844 Collezione di Studi Fenici, 46. Fabrizio Serra Editore, Pisa-Roma, Italy, pp. 251-263.

845 Zazo, C., Goy, J.L., Lario, J., Silva, P.G., 1996. Littoral zone and rapid climatic changes during the last 20 000
846 years. The Iberian Study case. Zeitschrift für Geomorphol. 102, 119-134.

847 Zazo, C., Silva, P.G., Goy, J.L., Hillaire-Marcel, C., Ghaleb, B., Lario, J., Bardajı´, T., González, A., 1999.
848 Coastal uplift in continental collision plate boundaries: data from the Last Interglacial marine terraces of the
849 Gibraltar Strait area (south Spain). Tectonophysics 301, 95-109.

850 Zazo, C., Dabrio, C. J., Goy, J. L., Lario, J., Cabero, A., Silva, P. G., Bardaji, T., Mercier, N., Borjag, F.,
851 Roquero, E., 2008. The coastal archives of the last 15 ka in the Atlantic-Mediterranean Spanish linkage area:
852 Sea level and climate changes. Quat. Int. 181, 72-87.

853

854

855

856

857

858

859

860

861

862

List of Figures

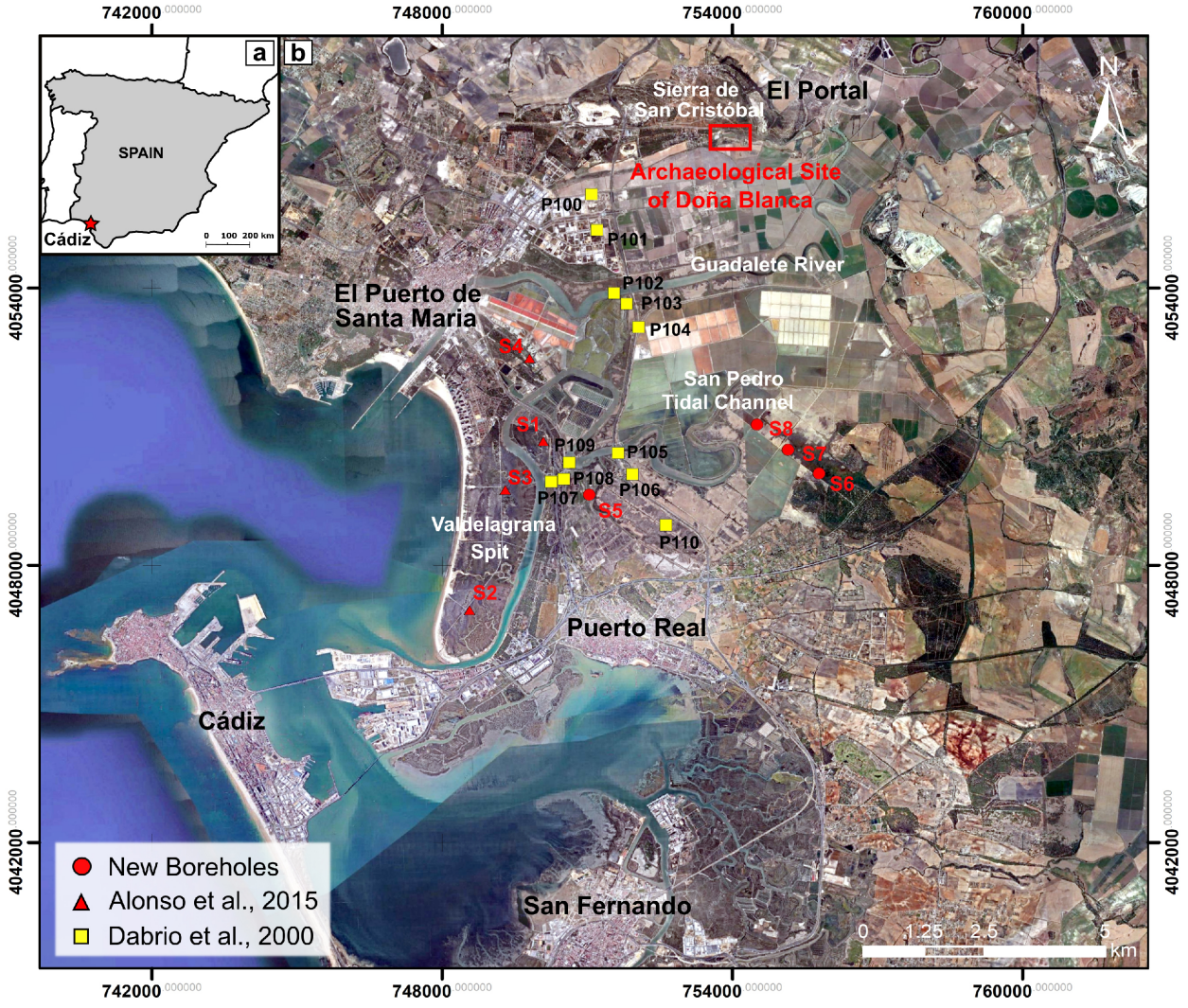

Figure 1. a: location map of the study area; b: the Northern Bay of Cadiz and boreholes drilled in the zone (Google Earth, 2020).

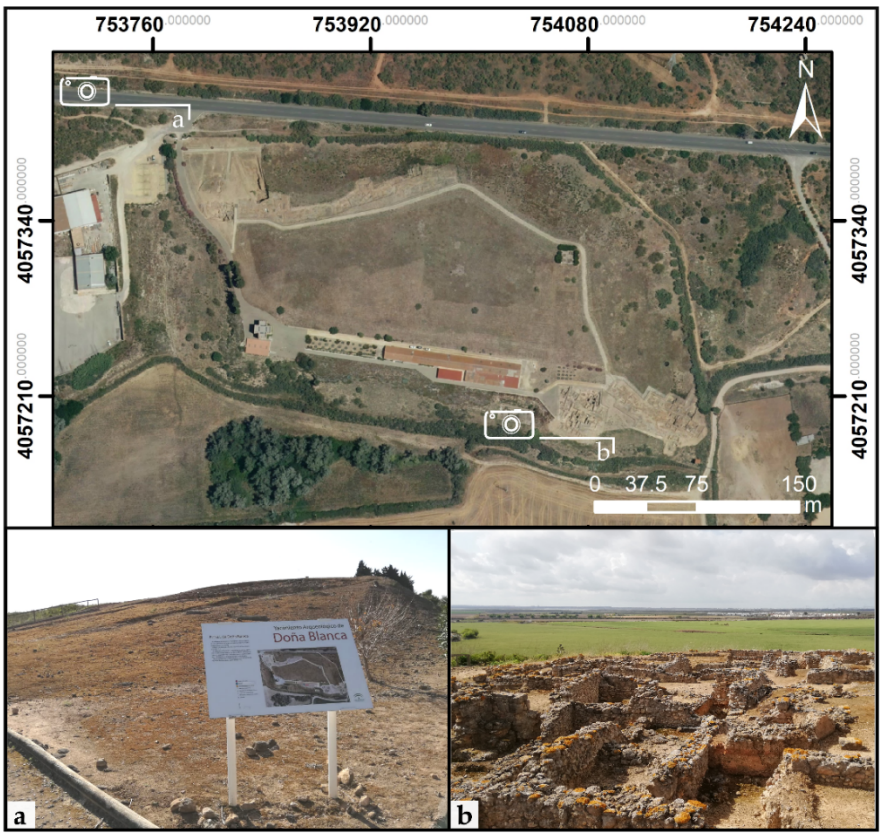

Figure 2. Doña Blanca archaeological site; a: detail of the entrance; b: detail of the ruins facing the Northern Bay of Cádiz.

Figure 3. a: location map of the surveyed area; b: flight plan performed during the UAV survey at Doña Blanca.

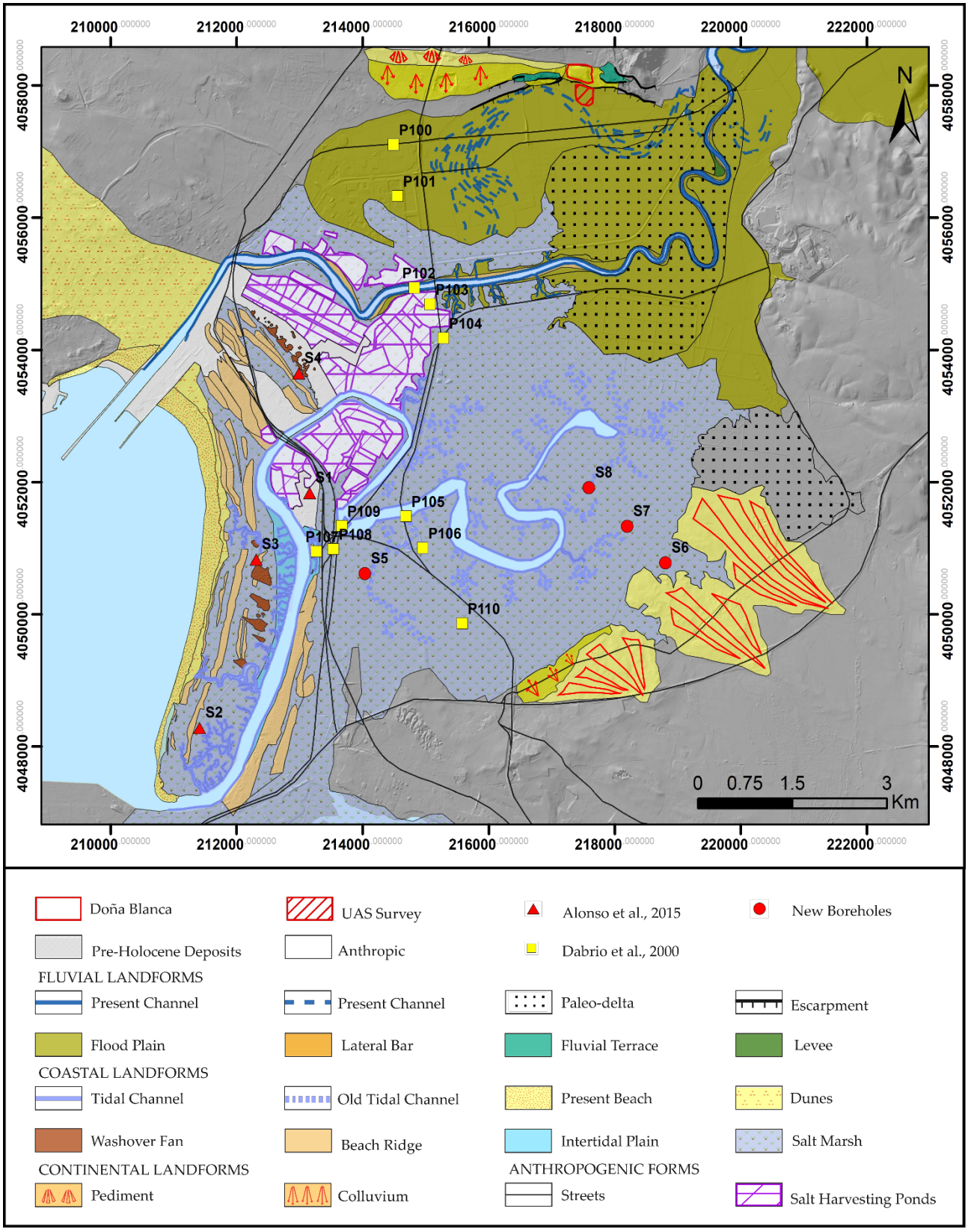

Figure 4. Simplified geomorphological map of the Northern Bay of Cádiz.

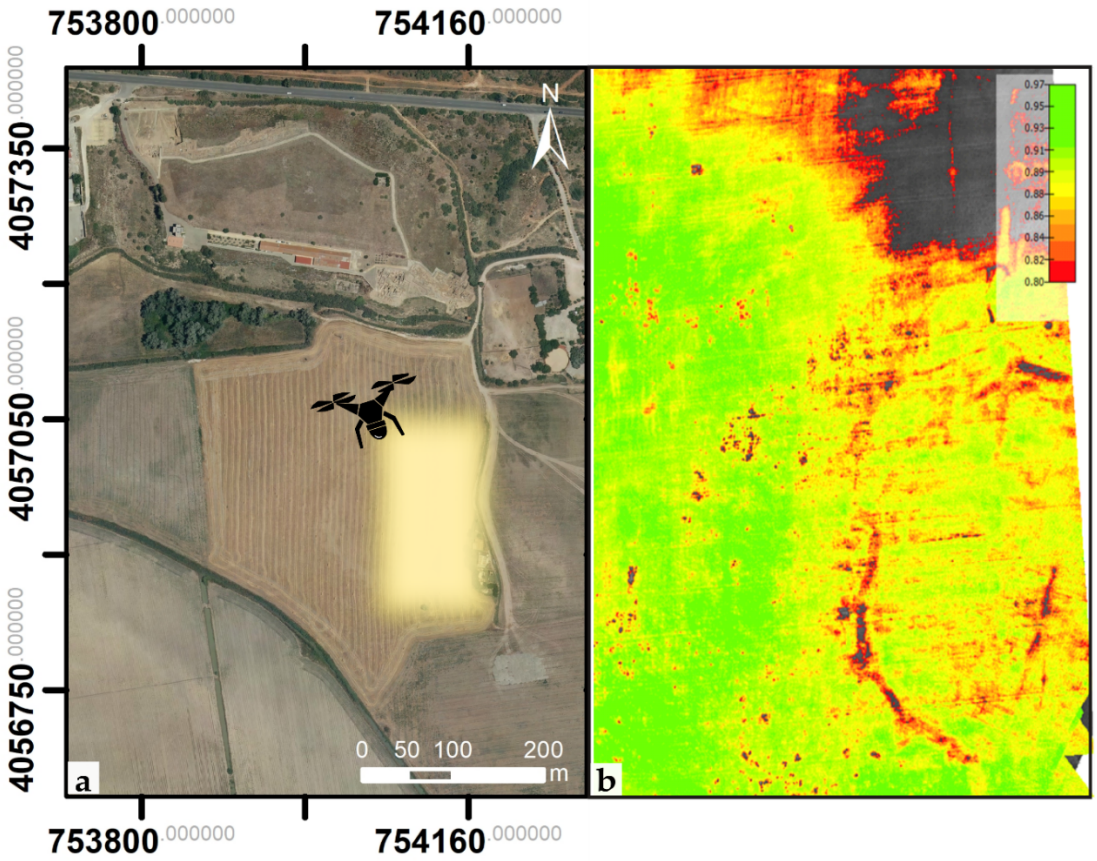

Figure 5. a: location map of the area subject to the drone multispectral investigation; b: normalised difference vegetation index (NDVI) in which structures reflecting differences in the vigour of the plants can be clearly observed. Subhorizontal lines represent the trace of the crop NDVI scale from 0,8 to 0,97.

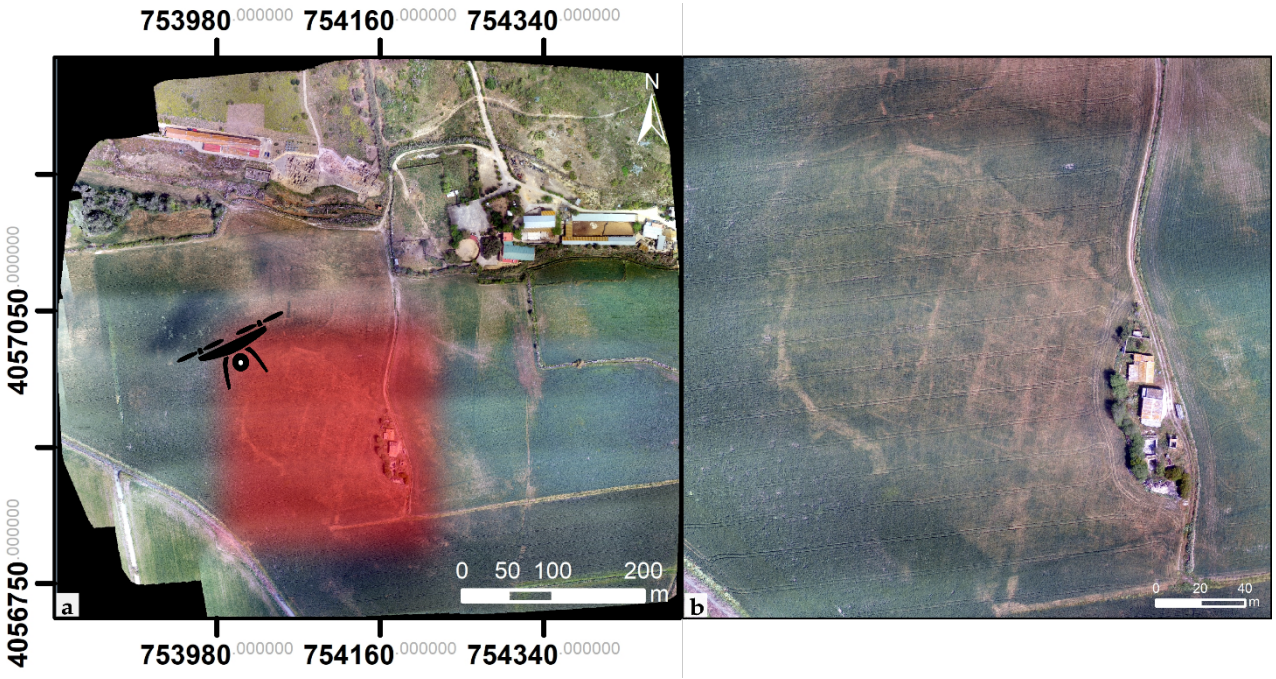

Figure 6. a: location map of the area subject to the topographic mapping; b: orthomosaic obtained after processing of 370 RGB images taken at 90 m of altitude over the vicinity of Doña Blanca archaeological site.

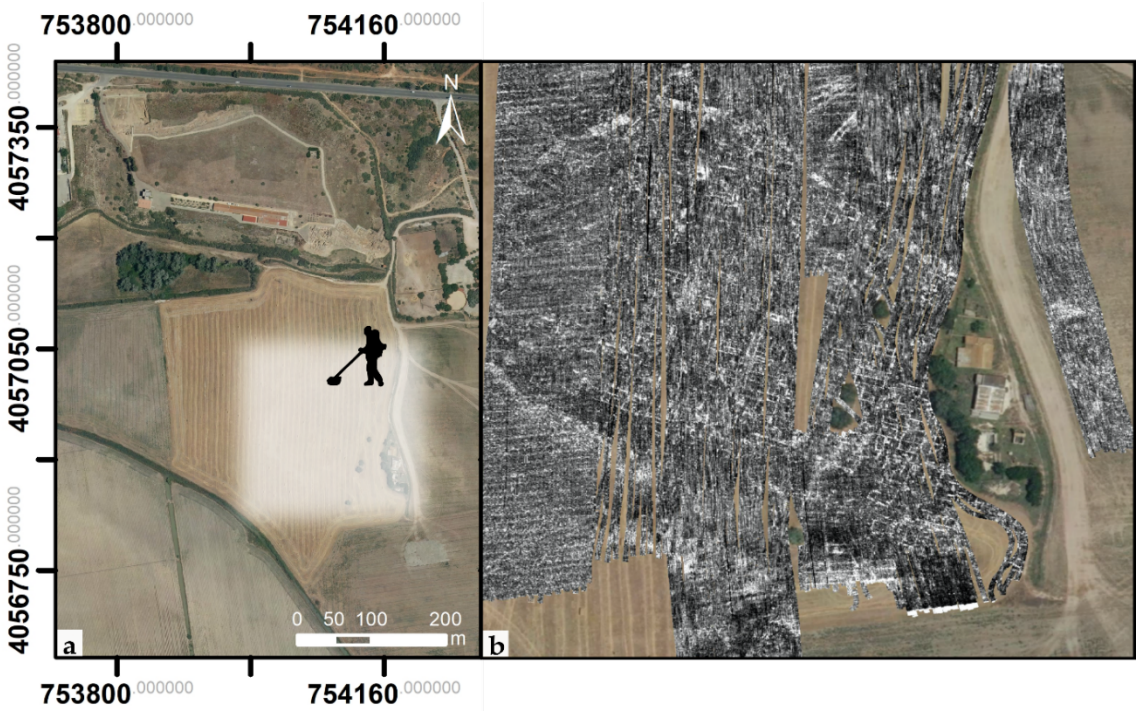

892

893 **Figure 7.** a: location of the area subject to the georadar survey; b: GPR results of the settlement at -50 cm
894 detected in 2016 (modified from Lagóstena and Ruiz, 2020). A complex structure of streets and houses can be
895 identified inside the walled site.

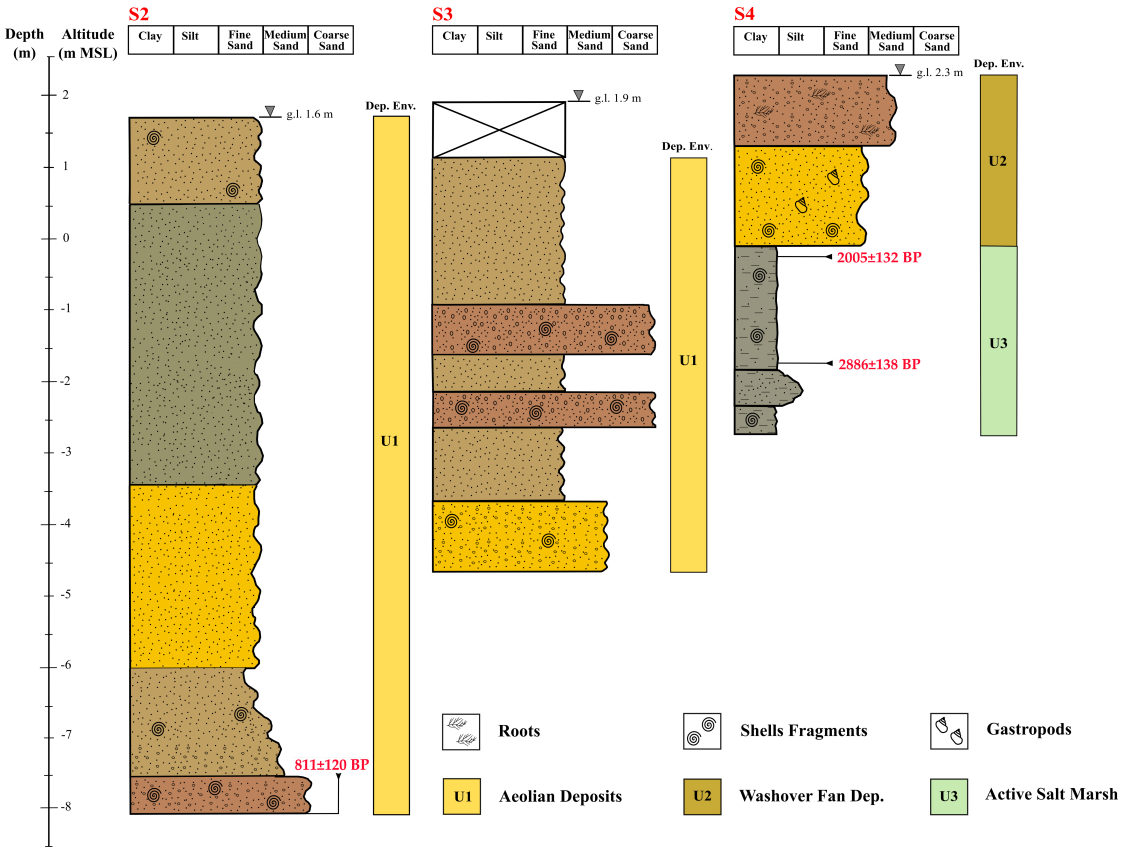

896

897 **Figure 8.** Schematic stratigraphic logs of the boreholes S2, S3 and S4, modified from Alonso et al., 2015 (for
898 location see Figure 1).

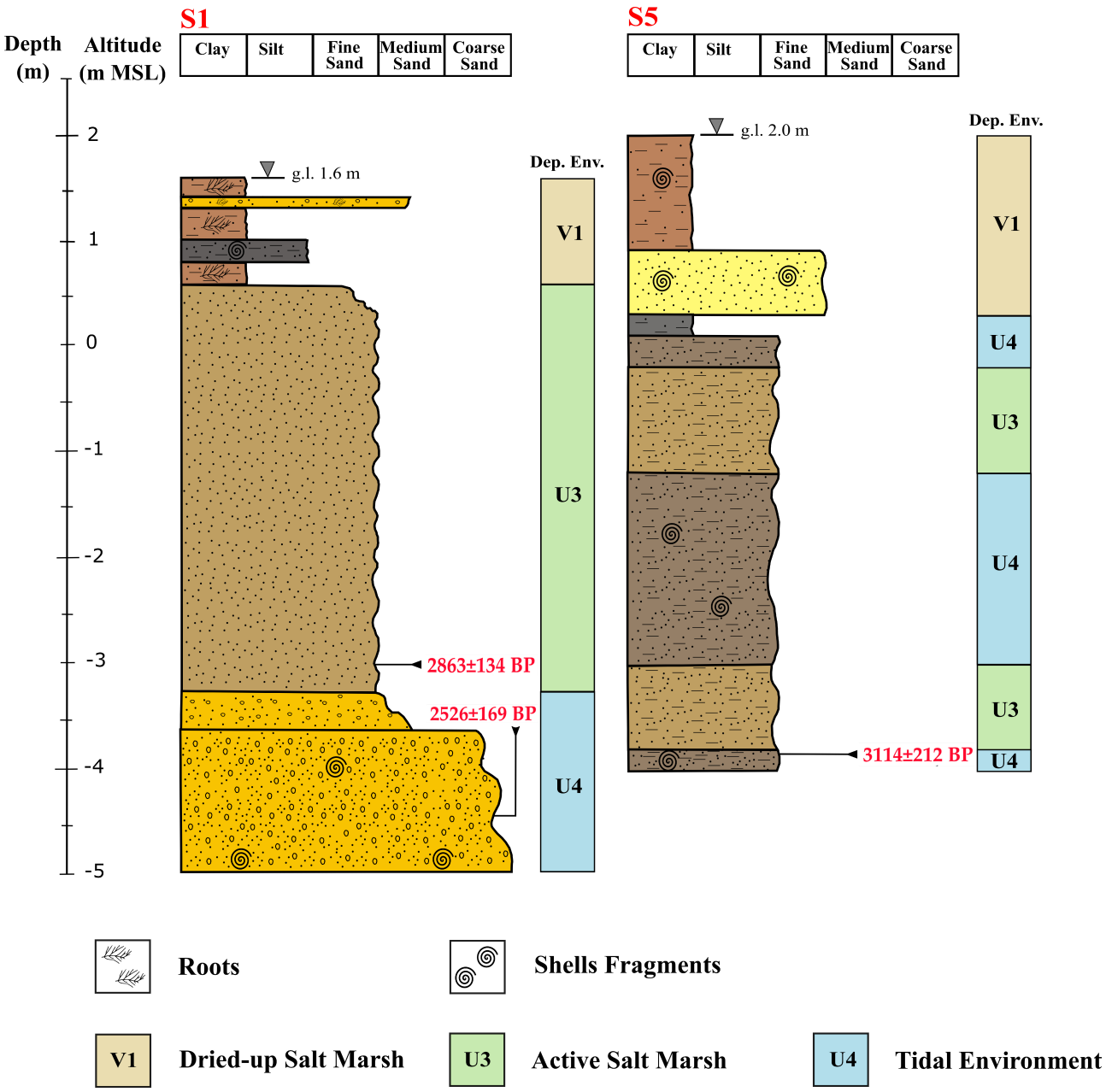

Figure 9. Schematic stratigraphic logs of the borehole S1 (modified from Alonso et al., 2015) and the new drilling S5 carried out in the Northern Bay of Cádiz (for location see Figure 1).

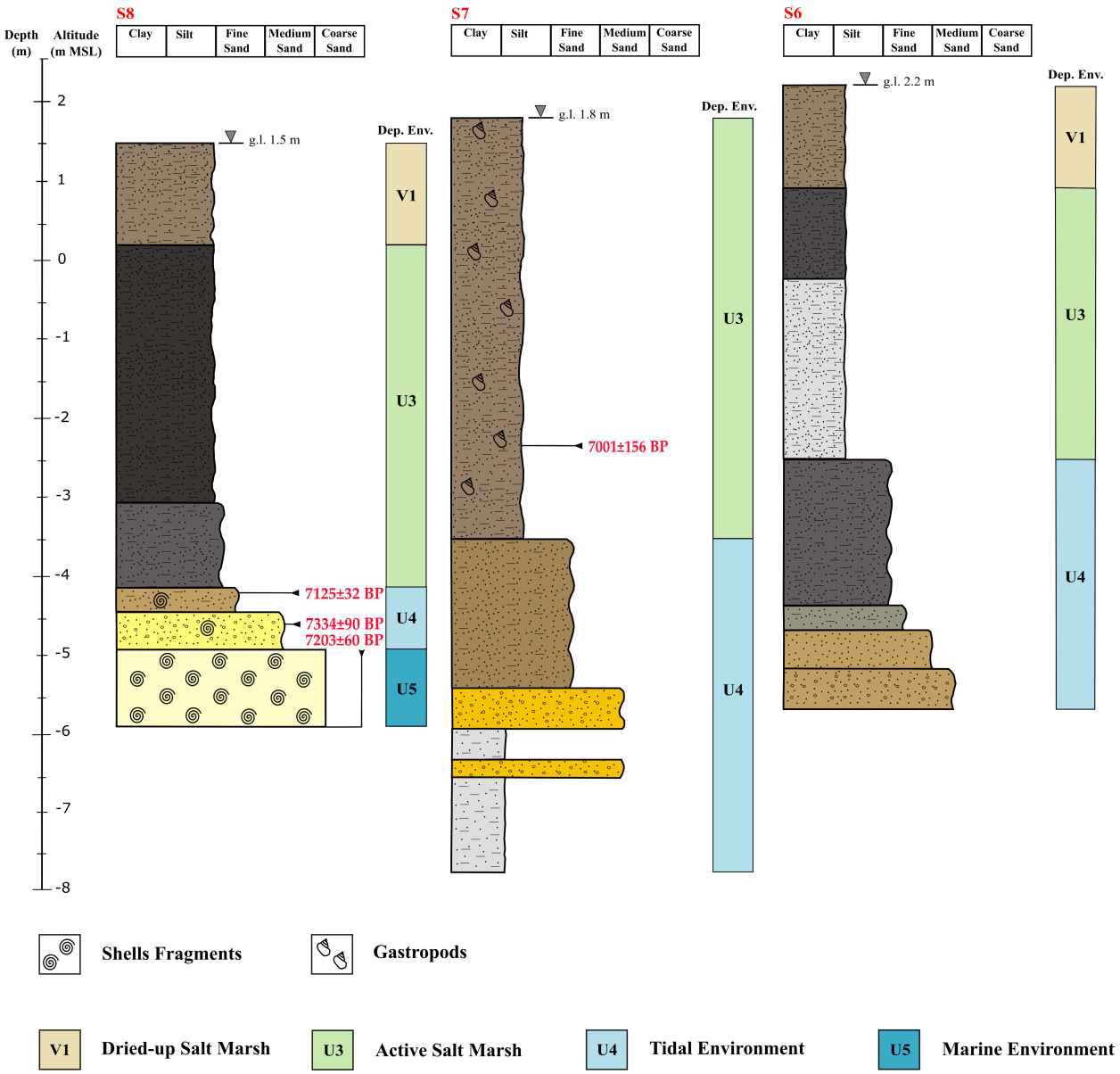

Figure 10. Schematic stratigraphic logs of the new drillings carried out in the Northern Bay of Cádiz (for location see Figure 1).

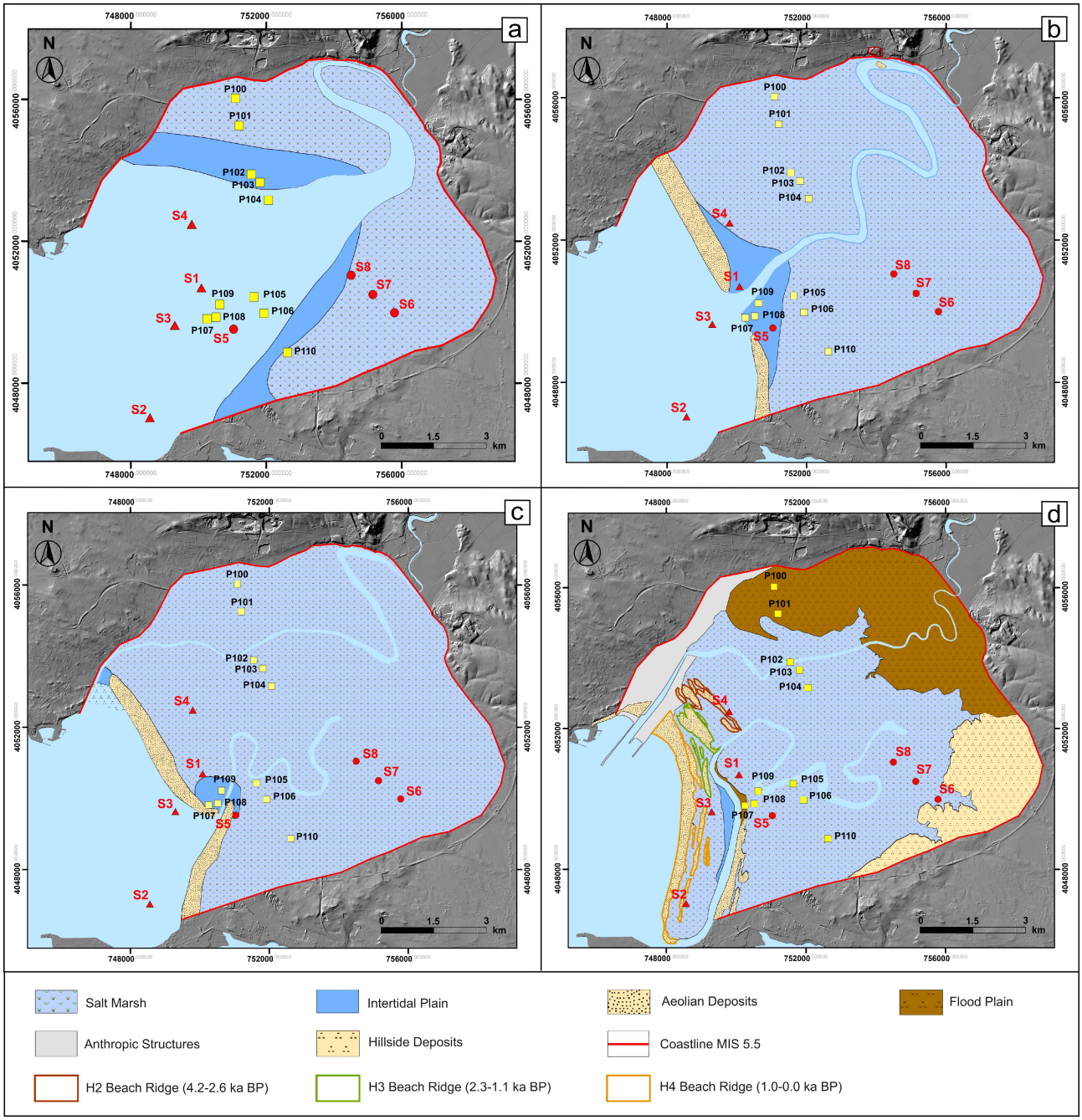

Figure 11. Palaeogeographic evolution proposal for the northern Bay of Cádiz. a: scenario related to 6.5 ka BP; b: scenario related to 3.0 ka BP; c: scenario related to 2.0 ka BP; d: scenario related to the present day.

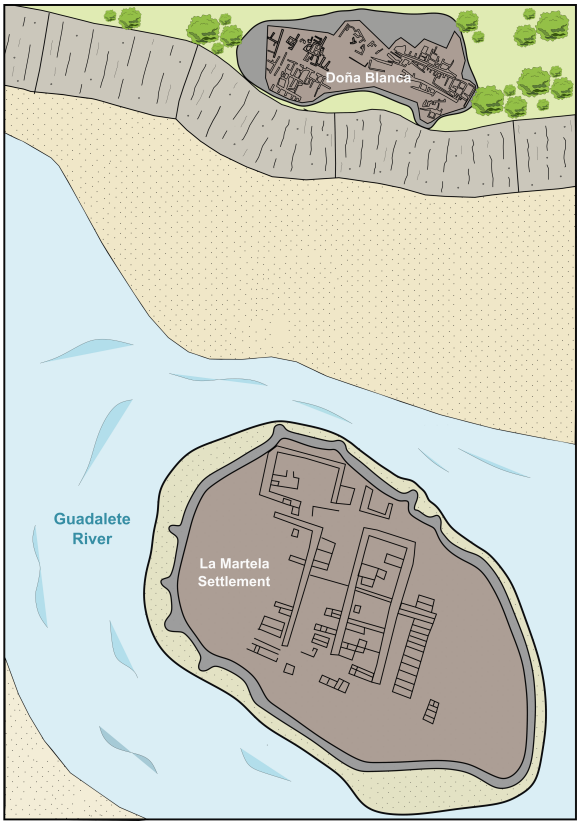

Figure 12. Palaeogeographic scenario of Doña. Blanca around 2.7-2.5 ka BP.

944 **List of Tables**

945 **Table 1**. Description of the stratigraphy of the cores obtained in Valdelagrana Spit. Modified from Alonso et
946 al. (2015).

Cores	Sedimentary Units	Lithofacies	Environmental Interpretation
S2	U1	Light brown fine sands with not abundant remains of shells. Increasing grain size at the transition to level 2.	Aeolian sands
		Grey fine sands. No remains of organisms.	Aeolian sands
		Yellow fine sands. No remains of organisms.	Aeolian sands
		Fine sands with remains of shells similar to the level 1. Coarsening upward.	Beach
		Sands with abundant very small fragments of macro-fauna.	Beach
S3	U1	Light brown fine sands. No remains of organisms.	Aeolian sands
		Coarse-grained sands with abundant macro-fauna bioclasts.	Washover fan (high energy)
		Yellow sands with shell remains.	Beach
S4	U2	Brown sands with remains of roots. Low content of water. Present soil.	Aeolian dune
		Yellow fine sands with abundant remains of marine bivalves, gastropods and other organisms.	Beach
	U3	Grey clays with remains of herbal organic matter and foraminifer shells.	Active saltmarsh
	U4	Silty clays with organic remains of amorphous aquatic material and coal.	Tidal plain with fluvial influence

947
948
949
950
951
952
953
954
955
956
957
958
959
960

961 **Table 2.** Description of the stratigraphy of the boreholes performed in the inner side of the Bay.

Cores	Sedimentary Units	Lithofacies	Environmental Interpretation
S1	V1	Dark brown clays with remains of thin roots and amorphous aquatic material. Coarsening upward.	Dried-up saltmarsh
		Yellow sands with remains of roots similar to level 1. Finning upward.	Dried-up saltmarsh
		Grey sandy muds with shells remains. Finning upward.	Dried-up saltmarsh
	U3	Brown muddy sands with no remains of organic matter. Coarsening upward in the first 30 cm and subsequent homogeneity.	Active saltmarsh
	U4	Yellow sands similar to the previous level but with a different colour that may represent a transitional period.	Transitional facies
		Coarse-grained sands with visible quartz grains. Abundant shell macro-fragments. Rounded grains of small size at the base, finning upward.	Sandy beach
S5	V1	Brown clays with macro-fauna remains (shells). Coarser grains at the base.	Dried-up saltmarsh
		Dark yellow fine sands with shell remains.	Energetic event
	U3	Greyish clays.	Tidal channel
		Dark brown muddy sands.	Tidal channel
	U4	Muddy sands without macro-fauna remains.	Active saltmarsh
S6	V1	Very fine muds with dark brown colour and high content of amorphous organic matter and micro-carbonates. Presence of very small grains of quartz.	Dried-up saltmarsh
	U3	Very fine dark grey muds. Higher quartz content and less organic matter than in the previous level. Strong sulphurous smell that may indicate breakdown processes of organic matter.	Active saltmarsh
		Very fine light grey muds with lower content of quartz and organic matter than level 1.	Active saltmarsh
	U4	Dark grey sandy muds with content of organic matter less than 5%.	Tidal channel
		Grey-brown muddy sands.	Tidal channel
		Light brown fine sands with small clasts.	Fluvial influence
		Sands with a higher content of coarser, rounded clasts than previous facies.	Fluvial influence
S7	U3	Dark brown fine muds with abundance of gastropods. From a depth of 250 cm the number of gastropods decreases progressively.	Active saltmarsh
	U4	Muddy sands that become reddish at a depth of 580 cm. Increasing grain-size sequence of 2 cm at the base.	Tidal channel
		Not very consolidated yellow sands.	Tidal plain with fluvial influence
		Level of white carbonate with small clasts.	Tidal plain with fluvial influence
		Well consolidated light grey muds.	Tidal plain with fluvial influence
S8	V1	Light brown muds.	Dried-up saltmarsh
	U3	Dark grey muds with a 2 cm thick coarser layer. Finning upward sequence in the last 5 cm.	Active saltmarsh
		Dark grey sandy muds.	Lower saltmarsh
	U4	Muddy sands with macro-fauna remains (shells).	Transition to tidal channel
		Dark brown sands with abundant fragmented remains of macro-fauna.	Tidal channel
	U5	Mostly intact shells, finning upward.	Marine environment

962

963

964

965

966

967

968

969

970 **Table 3.** Radiocarbon dating results.

Sample	Unit	Dated Features	Depth (m)	Conventional Radiocarbon Age	Calibration 2σ (95%)	Calibrated Age (yr BP)	Reference
S1_a1	U1	Shells	6.0	2615±50 BP	2695-2357 BP	2526±169	Alonso et al., 2015
S1_a2	U3	Shells	4.8	2895±50 BP	2997-2729 BP	2863±134	Alonso et al., 2015
S2_a1	U1	Shells	9.5	1170±50 BP	691-931 BP	811±120	Alonso et al., 2015
S4_a1	U3	Shells	4.0	2995±45 BP	2748-3025 BP	2886±138	Alonso et al., 2015
S4_a2	U3	Shells	2.5	2270±40 BP	1873-2137 BP	2005±132	Alonso et al., 2015
S5_a1	U4	Shells	5.8	3100±70 BP	3326-2902 BP	3114±212	New data
S7_a1	U3	Gastropods	5.0	6090±50 BP	7157-6845 BP	7001±156	New data
S8_a1	U5	Shells	7.5	6240±45 BP	7262-7143 BP	7203±60	New data
S8_a2	U4	Shells	6.1	6380±50 BP	7424-7244 BP	7334±90	New data
S8_a3	U3	Shells	5.7	6090±45 BP	7156-7093 BP	7125±32	New data

971